Pharmaceutical Research, Vol. 26, No. 5, May 2009 (© 2008)
DOI: 10.1007/s11095-008-9728-7

Research Paper

Prediction of Vitreal Half-Life Based on Drug Physicochemical Properties: Quantitative Structure–Pharmacokinetic Relationships (QSPKR)

Chandrasekar Durairaj,[1] Jaymin C. Shah,[3] Shruti Senapati,[4] and Uday B. Kompella[1,2,5]

Received May 7, 2008; accepted September 11, 2008; published online October 8, 2008

Purpose. The aim of this study was to develop quantitative structure pharmacokinetic relationships (QSPKR) to correlate drug physicochemical properties (molecular weight, lipophilicity, and drug solubility), dose, salt form factor, and eye pigmentation factor to intravitreal half-life in the rabbit model.
Methods. Dataset derived from prior literature reports, which included molecules with complete structural diversity, was used to develop the QSPKR models. Entire dataset as well as subsets limited to albino rabbit data, pigmented rabbit data, acids, bases, zwitterions, neutral compounds, suspensions, and macromolecules were analyzed. Multiple linear regression analysis was carried out with noncollinear independent variables and the best-fit models were selected based on correlation coefficients and goodness of fit statistics.
Results. The analysis indicated that logarithm of MW (Log MW), lipophilicity (Log *P* or Log *D*) and dose number (dose/solubility at pH 7.4), are the most critical determinants of intravitreal half-life of the compounds analyzed. The best-fit models obtained from the entire dataset (Log $t_{1/2}$=−0.178+0.267 Log MW−0.093 Log *D*+0.003 dose/solubility at pH 7.4+0.153 Pigmentation Factor and Log $t_{1/2}$=−0.32+0.432 Log MW−0.157 Log *P*+0.003 dose/solubility at pH 7.4) predicted the various subsets well. Pigmented dataset and zwitterions were better predicted by Log *P* rather than Log *D*.
Conclusions. The present study confirmed that intravitreal half-life could be better predicted by a group of variables (Log MW, Log *P* or Log *D*, dose number) rather than a single variable. In general, increasing Log MW and dose number, while reducing Log *D* or Log *P* would be beneficial for prolonging intravitreal half-life of drugs.

KEY WORDS: half-life; intravitreal; pharmacokinetics; quantitative structure–pharmacokinetic relationship (QSPKR); rabbits.

INTRODUCTION

Age-related macular degeneration, diabetic retinopathy, retinitis pigmentosa, optic nerve damage associated with glaucoma, and bacterial/fungal endophthalmitis are some of the vision impairing conditions afflicting the posterior segment of the eye (1). The exposure of affected target tissues to therapeutic quantities of drugs for appropriate lengths of time is an enormous challenge faced in the successful treatment of these conditions. Topical, systemic, and periocular routes of administrations are limited by their systemic side effects and solute permeability limitations (2). Intravitreal injections, providing more efficient drug delivery to the back of the eye compared to the above routes, are effective for a wide range of therapeutics including low molecular weight drugs as well as macromolecules. Beneficial effects have been shown in humans for a variety of drugs including low molecular weight drugs (3), oligonucleotides (Fomivirsen®) (4), and monoclonal antibodies or their fragments (Avastin® and Lucentis®) (5). The duration of effects of an intravitreally administered drug depends on the retention of the injected drug at the site of administration. The higher the intravitreal half-life of a drug injected in the vitreous of the eye, the greater is the anticipated duration of the pharmacological response. Longer half-life of a drug makes it amenable for less frequent dosing. However, it is time consuming and cost intensive to determine the intravitreal half-life of drugs *in vivo*. A scientific understanding of the relationship between physicochemical properties such as molecular weight (MW), lipophilicity, and solubility and drug elimination is essential for the development of therapeutic agents with desired intravitreal pharmacokinetic (PK) properties.

Quantitative structure–pharmacokinetic relationship (QSPKR) approaches attempt to derive relationships between the molecular properties of drugs and their PK properties. Once a validated model is developed, it might be useful in predicting PK parameters of a new compound or in selecting a molecule with desired PK properties from a library

[1] Department of Pharmaceutical Sciences, University of Colorado Denver, 4200 East 9th Avenue, C-238, Denver, CO 80262, USA.
[2] Department of Ophthalmology, University of Colorado Denver, Denver, CO 80262, USA.
[3] Pfizer Global Research and Development, Groton, CT 06340, USA.
[4] Biomedical Engineering, Georgia Institute of Technology, Atlanta, GA, USA.
[5] To whom correspondence should be addressed. (e-mail: Uday.Kompella@UCHSC.edu)

of compounds. Such an approach, serving as an initial screen for compounds, is expected to minimize the animal use. Recent years have witnessed a steep rise in the QSPKR based approaches to establish the relationship between the physicochemical/molecular properties and various PK parameters such as volume of distribution (6) and clearance (7). In addition, QSPKR had been used to predict the aqueous solubility (8) and plasma protein binding (9) of drug molecules.

In ocular drug delivery, QSPKR type of analysis was attempted to correlate physicochemical properties to drug permeation across cornea (10–14), conjunctiva (12,15,16), sclera (12), and retinal pigment epithelium (17). Maurice (18,19) was the first to study the QSPKR in vitreous humor. His group established the relationship that high molecular weight (MW) compounds have a high aqueous/vitreous ratio indicating the elimination of compounds by way of the anterior chamber. Also, there were few reports aimed at understanding spatial–temporal distribution of drug in the vitreous using mathematical modeling and computer simulations (20–25). These studies aimed at simulating the diffusion and distribution of the drug in the vitreous humor after intravitreal injection.

A systematic study was carried out by Miller (26) to correlate the physicochemical properties and drug elimination from vitreous following intravitreal injection. These authors had shown an excellent correlation between lipophilicity (Log *D* at pH 7.2) and vitreal elimination half-life following intravitreal injection in albino rabbits. However, the QSPKR was developed using a small set of structurally similar molecules (ciprofloxacin, fleroxacin, ofloxacin, and sparfloxacin). In addition, there were some investigational efforts to correlate drug elimination with MW (27,28). Dias and Mitra (27) had shown an inverse relationship between the Log MW and vitreous elimination rate constant for high MW hydrophilic compounds (FITC–dextrans). Maurice (28) reported computer-generated concentration contours for the diffusional loss of drugs from the human vitreous and demonstrated that the vitreal half-lives of compounds increased with increasing MW. Thus, some previous reports indicated the dependence of vitreal half-life on MW or lipophilicity. The earlier QSPKR studies for vitreal elimination half-life based on a small set of chemically similar molecules limits their application to predict half-lives of structurally different molecules. The objective of the present study was to develop a QSPKR based model with diverse unrelated compounds from the available literature reports and to understand the influence of some important physicochemical properties including MW, lipophilicity, and solubility on intravitreal elimination half-life.

METHODS

Data Collection for Intravitreal Half-Lives of Solutes

Literature search was conducted using the database PubMed (1966–May 2007) to identify prior literature reports for analysis. Search terms included ‘intravitreal’, ‘vitreal’, ‘pharmacokinetics’, ‘elimination’, ‘half-life’, and ‘clearance’. Reference lists from all retrieved articles were also reviewed and citations were retrieved if they referred to intravitreal pharmacokinetics. Since most of the literature reported intravitreal half-life of molecules in rabbits (few in human and other species), data pertaining to studies conducted exclusively in rabbits were considered for analysis. Data from both albino (more commonly assessed) strain as well as pigmented rabbit strain was collected. Although not likely complete, we believe we captured majority of the literature reports related to vitreal half-life in this study. From literature reports, besides half-life, other data concerning the drugs including the salt form administered, injected dose, injection volume, and dosage form (solution or suspension) was also collected.

In most of the earlier literature reports, investigators estimated the elimination half-life of the compounds using a few time points without any compartment modeling. The half-lives estimated using this noncompartmental approach was listed in the tables as terminal/elimination half-life. Half-lives estimated in literature reports using one compartment model was listed as half-life based on K_{10} (the only elimination rate constant from one-compartment model). In case of two compartment models, any reported half-lives including distribution half-life or $t_{1/2,\alpha}$, elimination half-life or $t_{1/2,\beta}$, and $t_{1/2,K10}$ or half-life for elimination from the central compartment were tabulated.

Pharmacokinetic Analysis of Some Literature Reported Concentration–Time Profiles

For literature reports with full concentration–time course data and limited detail on the relevant half-lives, pharmacokinetic analysis was carried out in this study using WinNonlin (version 1.5, Pharsight Inc., CA) to determine the PK parameters. The concentration–time data were fit to different PK models, and the best fit model was selected on the basis of the correlation coefficients and Akaike Information Criterion (AIC) values. Estimated half-life values for these drugs were compared with the literature reported values and used for regression analysis.

Collection of Molecular Descriptors

MW, Log *P*, Log *D* at pH 7 (hereafter mentioned only as Log *D*) and intrinsic solubility (IS) for the listed compounds were collected from SciFinder Scholar, which reports values calculated using Advanced Chemistry Development (ACD/Labs) Software V8.14 for Solaris (1994–2007 ACD/Labs). Solubility at pH 7.4 for all the molecules was estimated using ACD/I-Lab Web service (ACD/Aqueous solubility 8.02). For macromolecules with no reported molecular descriptors in SciFinder Scholar, wherever available, literature reported values for MW, lipophilicity, and solubility were collected. Logarithmic transformation was carried out for those variables showing broad range or high standard deviation (MW, intrinsic solubility, solubility at pH 7.4 and half-life).

Model Construction

Selection of Independent Variables

Since the dataset included half-lives from albino and pigmented rabbits, a dummy variable pigmentation factor (PF) denoting 0 for albino and 1 for pigmented was included in the analysis. Also a dummy variable salt factor (SF) was

included denoting 0 for non-salt form of molecules and 1 for molecules administered in the salt form. To understand the effect of dose administered on the vitreal disposition of molecules, a new variable dose number (DN=dose injected/solubility at pH 7.4) was included as an independent variable in the analysis. For regression analysis, the variables collected were divided into two sets: the first set included Log MW, Log *D*, DN, PF and SF. The second set included Log MW, Log *P*, DN, PF and SF. Multicollinearity (condition that exists when independent variables are highly correlated with each other) was tested for each set by evaluating the relationship between the above variables using the correlation matrix (SPSS 11.5, SPSS Inc., IL). Two variables were considered collinear, if the correlation coefficient (*R*) between them was greater than 0.5.

Multiple Regression Analysis of Data for Model Development

Multiple linear regression analysis of the selected non-collinear independent variables was performed to determine statistically significant relationships between the variables and vitreal half-life using SPSS 11.5 (SPSS Inc., IL) statistical software. Half-life from both the strains was included for regression analysis only if the difference in half-lives were greater than 5 h. In order to determine the individual contributions of the predictor variables and to attain a best predicting model, backward stepwise regression was used to develop the model. In this model, all variables were fit first, and then the non-significant variables were removed one at a time until all the remaining variables in the model contribute significantly to the regression equation. At each step, the variable with the smallest contribution to the model (highest *P* value) was removed until the *P* value was less than 0.05. The above procedure was undertaken for (1) the entire dataset (all), (2) albino, (3) pigmented, (4) acids, (5) bases, (6) zwitterions, (7) neutrals, (8) suspensions, (9) macromolecules, (10) all without suspensions, (11) all without macromolecules, (12) salts, and (13) all without salts.

From the various models generated with each group, the best-fit model was selected based on the goodness-of-fit statistical parameters—high R^2, larger *F* values, and lowest *P* value. Only cases with valid values for all variables were included in the analysis. Since the data set included different half-lives, regression analysis was done in two different ways. First, regression analysis was done using $t_{1/2,\beta}$ from two-compartment models, $t_{1/2,\text{terminal/elimination}}$ from non-compartmental analyses, and $t_{1/2,\text{K10}}$ for one-compartment models. Second, wherever full time course data is available for drugs obeying two-compartment model, beta half-lives were replaced with their K_{10} half-lives. The half-lives exhibiting good correlation with the independent variables based on the statistical parameters were selected for model development. Outliers were identified based on the residual values obtained from the regression analysis. Only those outliers whose removal improved the correlation coefficient significantly were removed and the data reanalyzed.

Models for Subclasses of Compounds/Formulations

To better understand the vitreal elimination for compounds/formulations of various types, dataset was classified in five different ways. In the first classification, molecules were divided into two sets, albino and pigmented based on the rabbit strain used. In the second classification, molecules were divided as acids, bases, zwitterions and neutrals based on their p*K*a values. Based on the dose administered and its solubility, the third classification consisted of formulations separated as solutions and suspensions. If the dose administered (in grams per liter) exceeded the solubility of the compound, it was classified as a suspension. The fourth classification consisted of macromolecules (MW>1000) and all compounds without macromolecules (MW<1000). The fifth classification consisted salts and non-salt forms of the drugs. Multiple linear regression analysis was performed for each subset in a particular classification at a time. The best predicting model and the influencing variables were identified.

Validation of the Models

The best-fit model obtained from each subset was cross-validated against other subsets (e.g., albino equation assessed for its predictability of pigmented group, *etc.*). Also the best-fit model obtained from the entire dataset was tested for its predictive ability on various subsets.

RESULTS

Data Collection

Literature reports on vitreous half-life in rabbit models were identified for a total of 68 compounds. Of these, 49 were assessed in New Zealand white or albino rabbits and 19 were assessed in pigmented rabbits (11 were assessed in both). Table I summarizes the physicochemical properties of the compounds and their respective vitreal half-lives in New Zealand white rabbits. Table II summarizes the properties of compounds in pigmented rabbits. Compounds in both the datasets covered a wide range of structurally different molecules, with vitreal half-life values ranging from 0.87 to 218 h. The data set included molecules as small as methanol (MW 32) to macromolecules like bevacizumab (MW 149,000). The lipophilicity of the molecules spanned the entire range, from highly hydrophilic (Log *P*=−3.64 and Log *D*=−9.2) to highly lipophilic (Log *P*=3.44 and Log *D*=2.75) and the solubility ranged from 0.0018 to 31,722 g/L.

Pharmacokinetic Analysis of Data from Literature Reports

For 14 drugs (eight in albino; six in pigmented) for which entire concentration–time profile was available, pharmacokinetic analysis was carried out. Most of the drugs exhibited two compartments pharmacokinetics except gentamicin and methicillin in the albino group and etanercept and GSSG in the pigmented group. The literature reported vitreal half-life values ($t_{1/2,\text{terminal}}$ from noncompartmental analysis) were found close to the calculated K_{10} half-life values for most of the drugs except erythromycin in albino rabbits (Table III). Erythromycin exhibited two compartment kinetics with a beta half-life of 4.44 h against literature reported 10 h. In case of pigmented rabbits, significant differences were observed

Table I. Physicochemical properties and intravitreal half-lives of various solutes in New Zealand white (albino) rabbits

Drug	Molecular weight[a]	Log P[a]	Log D[a]	Solubility (g/L)		Vitreous $t_{1/2}$ reported (estimated)					Reference
				Intrinsic[a]	pH 7.4[b]	$t_{1/2,\alpha}$ (h)	$t_{1/2,\beta}$ (h)	$t_{1/2,\text{terminal}}$ (h)	$t_{1/2,\text{K10}}$ (h)	Reported method	
1-Heptanol	116.2	2.47	2.47	3	3.03			2.56		Noncompartmental	(35)
1-Pentanol	88.15	1.41	1.41	20	20.4			1.22		Noncompartmental	(35)
1-Propanol	60.1	0.34	0.34	98	98.2			0.98		Noncompartmental	(35)
Acyclovir	225.21	−1.76	−1.76	0.38	6.35		2.98			Two compartments	(36)
Amikacin	585.62	−3.343	−9.13	13	1,000	(1.64)	(26.04)	25.9	(25.82)	LS regression	(3)
Amphotericin B	924.08	1.21	−1.32	15	0.12			218.4		LS regression	(30)
Ampicillin	349.42	1.35	−1.54	0.07	1.22			6.5			(37)
Antiangiogenic peptide (A6)	911			455					19.4	One compartment	(38)
Carbenicillin	378.42	1.009	−3.74	0.13	1,000			5			(39)
Cefazolin	454.5	1.133	−2.53	0.0018	9.32	0.52‡	3.83‡		1.86†	One† or two‡ compartments	(40)
Ceftazidime	546.58[b]	−2.84[b]	−3.2[b]	125.21[b]	333[b]			7.4			(41)
Ceftriaxone	554.58	−0.249	−4	0.0061	0.54	(6.79)	(183.45)	12	(9.45)		(42)
Cephalexin	347.39	0.65	−2.2	0.11	3.3	0.21	3.09			Two compartments	(40)
Cephalothin	396.44	1.447	−2.2	0.021	108.9	0.6	2.44			Two compartments	(40)
Chloramphenicol	323.14	1.018	1.02	0.23	0.23			10			(3)
Cidofovir	279.19	−3.37	−7.11	293	1,000	20	41			Two compartments	(43)
Ciprofloxacin	331.3	1.313	−0.85	0.17	0.71			4.41		Noncompartmental	(26)
Clarithromycin lactobionate[c]	747.95	3.159	1.98	0.14	0.96			2			(44)
Clindamycin phosphate	504.96[b]	0.934[b]	−2.16[b]	0.76[b]	0.72[b]	(0.46)	(2.98)	3	(2.98)		(45)
Cyclosporine A	1,202.61[b]	3.35[b]	3.4[b]	4,678.7[b]	1,000[b]			10.8		Noncompartmental	(46)
Erythromycin gluceptate[c]	733.92	2.829	1.65	0.18	1.24	(0.31)	(4.44)	10	(0.47)		(47)
FITC–Dextran	4,400[b]	3[b]	0.4[b]	1.2[b]	19.8[b]				4.1	One compartment	(27)
FITC–Dextran	9,300[b]	3[b]	0.4[b]	1.2[b]	19.8[b]				4.58	One compartment	(27)
FITC–Dextran	38,900[b]	3[b]	−0.4[b]	1.2[b]	19.8[b]				8.07	One compartment	(27)
Fleroxacin	369.34	2.378	0.91	0.037	0.32				2.73	One compartment	(26)
Fluconazole	306.27	0.5	0.5	0.27	0.27	0.23	3.18			Two compartments	(48)
Fluorescein sodium[c]	376.27[b]	3.39[b]	0.9[b]	0.01[b]	4.72[b]			2.56		Noncompartmental	(49)
Foscarnet	126.01	−2.532	−7.48	665	1,000			34		Noncompartmental	(50)
Ganciclovir	255.23	−2.065	−2.07	0.43	5.73	0.72	7.1		2.83	Two compartments	(51)
Gentamicin	477.59[b]	−1.89[b]	−7.9[b]	12.28[b]	1,000			32	(32.77)	LS regression	(52)
Grepafloxacin	359.39	2.265	0.07	0.043	0.18			3			(53)
ISIS2922 (Fomivirsen)	7,122.16[d]					(2.16)	62 (63.46)		(29.27)	Two compartments	(54)
Kanamycin	484.5	−2.575	−7.47	10	1,000			18			(3)
Lincomycin	406.54	0.908	−0.85	0.41	10			10			(55)
Methanol	32.04	−0.72	−0.72	241	240.4			0.87		Noncompartmental	(35)
Methicillin	380.42	1.267	−2.42	0.099	522.4			3.5	(4.96)		(18)
Methotrexate sodium[c]	454.45	−0.241	−4.9	0.24	1,000				7.6	One compartment	(56)
Moxalactam	520.48	0.872	−3.88	0.029	1,000			20			(57)
Ofloxacin	361.37	1.607	−0.5	0.094	0.32			3.21		Noncompartmental	(26)
Oxacillin	401.44	2.054	−1.63	0.018	97.3			6			(3)
Penicillin G	334.39	1.667	−2.02	0.064	332.8			3			(3)
Quinidine HCl[c]	324.42	3.44	1.22	0.032	2.33			2.02		Noncompartmental	(58)

Rituximab	143,860[d]	−0.414[d]				112.8				Two compartments		(59)
Sparfloxacin	392.4	2.903	0.94	0.011	0.03		2.78			Nonccompartmental		(26)
Tobramycin	467.51	−3.409	−9.2	33	1,000				30	One compartment		(60)
Triamcinolone acetonide	434.5	0.833	0.83	0.15	0.021			69.4, 576 and 936				(31, 61)
Trifluorothymidine	296.2	0.074	−0.95	1.8	39			3.15				(62)
Vancomycin	1,449.25	−1.439	−4.7	1,000	49.8				21	One compartment		(63)
Voriconazole	349.31	0.927	0.93	0.23	0.23	(1.43)	(2.69)	2.5	(2.24)	LS regression		(64)

[a] Obtained from SciFinder Scholar using Advanced Chemistry Development (ACD/Labs) Software V8.14 for Solaris (1994–2007 ACD/Labs). Log *D* estimate was at pH 7.0
[b] The predicted values were obtained using the ACD/I-Lab Web service (8.02)
[c] Molecular descriptor values mentioned were for the non-salt (acid or base form) of the compound
[d] From reference (65)

between the reported and estimated half-life for foscarnet (77 *vs* 32.55 h) and vancomycin (62.34 *vs* 32.67 h). Multiple regression analysis was carried out using these estimated values.

Classification of Entire Dataset

Based on the acidic and basic p*K*a values, the molecules in the data set were divided into acids [13], bases [15], zwitterions [18] and neutrals [9] as shown in Table IV. Table V summarizes the physicochemical properties of 11 molecules administered in the suspension form. Molecules with MW> 1,000 are summarized in Table VI. Out of these ten macromolecules, all physicochemical properties could be obtained for only six molecules including three different MW ranges of FITC–dextrans. Other macromolecules with missing data were not included in the multiple regression analysis.

Multiple Linear Regression Analysis of Entire Data

Correlation matrix of all the predictor variables indicated that Log *D* and Log *P* are highly correlated (R=0.782, Table VII) with each other. The *R* values of all other variables were less than 0.5. Initial multiple linear regression analysis of the entire dataset using K_{10} half-lives (from both one and two compartments) as dependent variable yielded linear relationship with the independent variables (both Log *P* set and Log *D* set). On the other hand, models were not significant when terminal half-lives were used. Hence, further analysis was carried out by substituting K_{10} half-lives from one or two compartments, wherever feasible, along with terminal/elimination half-life for the rest of the compounds as the dependent variable. The results of the regression analysis along with the best-fit equations obtained and statistical parameters are summarized in Table VIII for Log *D* set of variables and in Table IX for Log *P* set of variables. Also the scatter plots of the best-fit models are shown in Fig. 1 (Log *D* set of variables) and Fig. 2 (Log *P* set of variables).

The best-fit models obtained from regression analysis of the entire dataset using Log *D* set of variables (Table VIII, Eqs. 1, 1a) or Log *P* set of variables (Table IX, Eqs. 1, 1a) indicated that amphotericin B and TA (both low dose (0.3 mg) and medium dose (4 mg) in albino group) were outliers. Correlation values (R^2) increased from 0.5 to 0.7 with the omission of above data for each drug, justifying their exclusion from the dataset. Further, influence analysis indicated the significance of TA high dose (16 mg) for the model. Also, exclusion of this observation decreased the R^2 values of models and hence it was retained in the dataset. Both the best-fit equations (Fig. 1a and Fig. 2a) included Log MW, Log *D* or Log *P* and DN as the contributing variables for half-life.

Models for Subclasses of Data

For regression analysis of the first classification, initially the albino group was subjected to backward regression analysis. Similar to the entire dataset, exclusion of amphotericin B and TA (both low dose (0.3 mg) and medium dose (4 mg) in albino group) improved the model-fits with high correlation (R^2=0.820 in the Log *D* variables set and 0.738 in

Table II. Physicochemical properties and intravitreal half-lives of various solutes in pigmented rabbits

Drug	Molecular weight[a]	Log P[a]	Log D[a]	Solubility (g/L)		Vitreous $t_{1/2}$ reported (estimated)					Reference
				Intrinsic[a]	pH 7.4[b]	$t_{1/2,\alpha}$ (h)	$t_{1/2,\beta}$ (h)	$t_{1/2,\text{terminal}}$ (h)	$t_{1/2,\text{K10}}$ (h)	Reported method	
Acyclovir	225.21	−1.76	−1.76	0.38	6.35			8.36		Noncompartmental	(36)
Aztreonam	434.44	−0.661	−5.43	0.15	1,000			7.5		LS regression	(66)
Bevacizumab	149,000[c]				25[c]		103.68			Two compartments	(67)
Carbenicillin	378.42	1.009	−3.74	0.13	1,000			5		LS regression	(68)
Cefazolin sodium[d]	454.5	1.133	−2.53	0.0018	9.32			7		Noncompartmental	(69)
Cefepime	480.55[b]	−1.62[b]	−1[b]	201.83[b]	119.1			14.3		Noncompartmental	(70)
Ceftazidime	546.58[b]	−2.84[b]	−3.2[b]	125.21[b]	333			20		Noncompartmental	(71)
Ceftizoxime	383.4	0.587	−2.98	0.031	146.3			5.7		LS regression	(71)
Ceftriaxone	554.58	−0.249	−4	0.0061	0.54			9.1		LS regression	(71)
Dexamethasone phosphate sodium[d]	472	0.65	−3.6	0.54	1,000			3.5		LS regression	(72)
Etanercept	51,235[e]	−0.529[e]							(145.23)	One compartment	(73)
Foscarnet	126.01	−2.532	−7.48	665	1,000	(8.85)	(323.65)	77	(32.55)	LS regression	(74)
Ganciclovir	255.23	−2.065	−2.07	0.43	5.73	(6.74)	(111.25)	8.66	(6.75)	LS regression	(74)
Gentamicin sulfate[d]	477.59[b]	−1.89[b]	−7.9[b]	12.28[b]	1,000[b]			24			(75)
Grepafloxacin	359.39	2.265	0.07	0.043	0.18			2.9		LS regression	(76)
GSSG (oxidized glutathione)	612.63	−0.938	−5.94	0.43	1,000				(11.47)	One compartment	(77)
Moxifloxacin	401.43	1.896	−0.63	0.044	0.12	(1.92)	(687.76)	1.72	(1.93)	LS regression	(78)
Triamcinolone acetonide	434.5	0.833	0.83	0.15	0.021			38		Noncompartmental	(32)
Vancomycin HCl[d]	1,449.3	−1.439	−4.7	1,000	49.8	(6.01)	(106.58)	62.34	(32.67)	Noncompartmental	(79)

[a] Obtained from SciFinder Scholar using Advanced Chemistry Development (ACD/Labs) Software V8.14 for Solaris (1994–2007 ACD/Labs). Log D estimate was at pH 7.0
[b] The predicted values were obtained using the ACD/I-Lab Web service (8.02)
[c] From reference (67)
[d] Molecular descriptor values mentioned were for the non-salt (acid or base form) of the compound
[e] From reference (73)

Table III. Vitreal half-lives estimated in this study based on some previous reports

Drug	Best-fit model[a]	Correlation coefficient (R^2)	Estimated $t_{1/2}$ (h)			Literature reported $t_{1/2,terminal}$ (h)[b]
			$t_{1/2,\alpha}$	$t_{1/2,\beta}$	$t_{1/2,K10}$	
Albino rabbits						
Amikacin	Two compartments	0.9994	1.64	26.04	23.10	25.9
Ceftriaxone	Two compartments	0.9694	6.79	183.45	9.45	12
Clindamycin phosphate	Two compartments	0.9994	0.46	2.98	2.98	3
Erythromycin gluceptate	Two compartments	0.987	0.31	4.44	0.47	10
Gentamicin	One compartment	1			32.77	32
ISIS 2922	Two compartments	0.9976	2.16	63.46	29.27	62
Methicillin	One compartment	0.9999			4.96	3.5
Voriconazole	Two compartments	1	1.43	2.69	2.24	2.5
Pigmented rabbits						
Etanercept	One compartment	0.9995			145.23	
Foscarnet	Two compartments	0.9868	8.85	323.65	32.55	77
Ganciclovir (dose=196 μg)	Two compartments	0.9983	1.13	6.98	6.98	7.14
Ganciclovir (dose=800 μg)	Two compartments	0.9887	6.74	111.25	6.75	8.66
GSSG (glutathione)	One compartment	0.9999			11.47	
Moxifloxacin	Two compartments	0.9999	1.92	687.76	1.93	1.72
Vancomycin	Two compartments	0.9653	6.01	106.58	32.67	62.34

[a] Pharmacokinetic analysis was done using WinNonlin software (version 1.5, Pharsight Inc., CA) using various models and the best-fit model was selected based on high correlation and low AIC (Akaike Information Criterion) values. Concentration *vs* time profiles used for analysis were obtained from the respective references (see Tables I and II)
[b] Half-life values reported in the respective references (see Tables I and II)

the Log *P* variables set; see equations 2 and 2a in Tables VIII and IX). In case of pigmented group, no statistically significant model was obtained with Log *D* variable set (Eq. 3, Table VIII). However, replacing Log *D* with Log *P* yielded a model with high correlation value (R^2=0.852, Fig. 2c) indicating the influence of Log *P* along with Log MW and DN in this group of molecules (Eq. 3, Table IX).

In the second classification, the best-fit equation obtained for acidic molecules indicated only Log *D* (Eq. 4, Table VIII; R^2=0.554) or Log *P* (Eq. 4, Table IX; R^2=0.435) as the influencing variable. However, both the equations had low correlation values. In case of bases, the best-fit equations obtained did not include Log MW (Eq. 5, Tables VIII and IX) and had high correlation values (R^2=0.930, Fig. 1k and R^2= 0.88, Fig. 2j). In case of zwitterions, exclusion of amphotericin B improved the model and the model included Log *D* (Eq. 6a, Table VIII) or Log *P* along with SF (Eq. 6a, Table IX) in the best-fit equations. The best-fit models developed for neutral molecules had only Log MW and DN in their equations with high R^2 values (0.904, Fig. 1m; Eq. 7 in Tables VIII and IX).

In the third classification, the best-fit models obtained for suspensions included Log MW and DN (Eq. 8, Table VIII) or

Table IV. Classification of the molecules in the data set as acids, bases, zwitterions, and neutrals

Acid	Base	Zwitterion	Neutral
Carbenicillin	Amikacin	Amphotericin B	1-Heptanol
Cefazolin (B)	Ciprofloxacin	Ampicillin	1-Pentanol
Cephalothin	Clarithromycin	Aztreonam (P)	1-Propanol
Dexamethasone phosphate (P)	Erythromycin	Cefepime (P)	Chloramphenicol
Fluorescein	Fluconazole	Ceftazidime (B)	Methanol
Foscarnet (B)	Gentamicin (B)	Ceftizoxime (P)	Triamcinolone acetonide (B)
Methicillin	Grepafloxacin	Ceftriaxone (B)	
Moxalactam	Kanamycin	Cephalexin	
Oxacillin	Lincomycin	Cidofovir	
Penicillin G	Moxifloxacin (P)	Clindamycin phosphate	
Trifluorothymidine	Quinidine	Fleroxacin	
	Sparfloxacin	GSSG (P)	
	Tobramycin	Methotrexate	
	Voriconazole	Ofloxacin	
		Vancomycin (B)	

(P) denotes that literature exists for data in pigmented rabbits and (B) denotes that literature exists for data in both albino and pigmented rabbits. For other molecules, literature data exists in albino rabbits

Table V. Physicochemical properties and intravitreal half-lives of various molecules administered as suspensions to albino or pigmented rabbits

Drug	Molecular weight[a]	Log P[a]	Log D[a]	Solubility (g/L)		Vitreous half-life (h)				Dose (mg)
				Intrinsic[a]	pH 7.4[b]	$t_{1/2,\alpha}$ reported (estimated)	$t_{1/2,\beta}$ reported (estimated)	$t_{1/2,\text{terminal}}$ reported (estimated)	$t_{1/2,\text{K10}}$ reported (estimated)	
Ampicillin	349.42	1.35	−1.54	0.07	1.22			6.5		0.5
Chloramphenicol	323.14	1.018	1.02	0.23	0.23			10		2
Fluconazole	306.27	0.5	0.5	0.27	0.27	0.23	3.18			0.1
Ganciclovir (B)	255.23	−2.065	−2.07	0.43	5.73	(6.74)	(111.25)	8.66	(6.75)	0.8
Grepafloxacin (P)	359.39	2.265	0.07	0.043	0.18			2.9		0.08
Moxifloxacin (P)	401.43	1.896	−0.63	0.044	0.12	(1.92)	(687.76)	1.72	(1.93)	0.2
Triamcinolone acetonide	434.5	0.833	0.83	0.15	0.021			69.4		0.3
Triamcinolone acetonide	434.5	0.833	0.83	0.15	0.021			576		4
Triamcinolone acetonide	434.5	0.833	0.83	0.15	0.021			936		16
Triamcinolone acetonide (P)	434.5	0.833	0.83	0.15	0.021			38		0.4

Molecules were classified as suspensions, if the injected dose (in milligrams) exceeded the solubility at pH 7.4. (P) denotes that literature exists for data in pigmented rabbits and (B) denotes that literature exists for data in both albino and pigmented rabbits

[a] Obtained from SciFinder Scholar using Advanced Chemistry Development (ACD/Labs) Software V8.14 for Solaris (1994–2007 ACD/Labs)

[b] The predicted values were obtained using the ACD/I-Lab Web service (8.02)

Table VI. Physicochemical properties and intravitreal half-lives of macromolecules (molecular weight>1,000)

Drug	Molecular weight[a]	Log P[a]	Log D[a]	Solubility (g/L)		Vitreous $t_{1/2}$ (h)			
				Intrinsic[a]	pH 7.4[b]	$t_{1/2,\alpha}$ reported (estimated)	$t_{1/2,\beta}$ reported (estimated)	$t_{1/2,\text{terminal}}$ reported (estimated)	$t_{1/2,\text{K10}}$ reported (estimated)
Bevacizumab (P)	149,000[c]				25[c]		103.68		
Cyclosporine A	1,202.61	3.35[b]	3.4[b]	4,678.7[b]	1,000				10.8
Etanercept (P)	51,235[d]	−0.529[d]							145.23
FITC–Dextran	4,400	3[b]	0.4[b]	1.2[b]	19.8				4.1
FITC–Dextran	9,300	3[b]	0.4[b]	1.2[b]	19.8				4.58
FITC–Dextran	38,900	3[b]	0.4[b]	1.2[b]	19.8				8.07
ISIS2922 (Fomivirsen)	7,122.16[e]					2.16	62 (63.46)	62	29.27
Rituximab	143,860[e]	−0.414[e]					112.8		
Vancomycin	1,449.25	−1.439	−4.7	1,000	49.8				21
Vancomycin (P)	1,449.25	−1.439	−4.7	1,000	49.8	(6.01)	(106.58)	62.34	(32.67)

(P) denotes that literature exists for data in pigmented rabbits

[a] Obtained from SciFinder Scholar using Advanced Chemistry Development (ACD/Labs) Software V8.14 for Solaris (1994–2007 ACD/Labs)

[b] The predicted values were obtained using the ACD/I-Lab Web service (8.02)

[c] From reference (67)

[d] From reference (73)

[e] From reference (65)

Table VII. Correlation matrix of the predictor variables

	Log MW	Log *P*	Log *D*	PF	SF	Dose/sol 7.4
Log MW	1.000	0.269	0.034	−0.020	0.138	−0.002
Log *P*	0.269	1.000	0.782	−0.312	0.084	0.041
Log *D*	0.034	0.782	1.000	−0.263	−0.107	0.155
PF	−0.020	−0.312	−0.263	1.000	0.136	−0.083
SF	0.138	0.084	−0.107	0.136	1.000	−0.074
Dose/sol 7.4	−0.002	0.041	0.155	−0.083	−0.074	1.000

Correlation matrix of all predictor variables used for regression analysis. Variables with correlation values>0.5 were considered collinear

Log MW, Log *P* and DN (Eq. 9, Table IX) in the equation. The equation obtained with Log *P* had high correlation (R^2=0.844, Fig. 2d) and in both the models of suspensions, all the doses of TA were included. The best-fit equation obtained for the dataset without suspensions indicated Log MW and Log *D* (Eq. 9, Table VIII) or Log MW and Log *P* (Eq. 9, Table IX) as the contributing variables for vitreal half-life. However, the R^2 values for these models were less (0.555). Exclusion of amphotericin B from these models improved the best-fit significantly in both the cases (R^2=0.705, Fig. 1e; R^2=0.646, Fig. 2e).

The equation obtained with macromolecules had high correlation value (R^2=0.980, Eq. 10, Tables VIII and IX) and included Log MW, PF and SF as the contributing variables. However, this group included only six molecules including FITC–dextrans of three different MW (Fig. 1f). Exclusion of macromolecules resulted in models including all three variables Log MW, DN and Log *D* (Eq. 11, Table VIII) or Log MW, DN and Log *P* (Eq. 11, Table IX). Exclusion of amphotericin B and TA low and medium doses from this dataset improved the correlation values significantly (R^2=0.720, Fig. 1g; R^2=0.731, Fig. 2f).

The best-fit model obtained from molecules administered in the salt form included Log MW and Log *D* (R^2=0.911, Eq. 12, Table VIII) or only Log *P* (R^2=0.909, Eq. 12, Table IX) as the independent variable contributing to the vitreal half-life. However, the exclusion of these molecules from the entire dataset resulted in inclusion of Log MW, DN and Log *D* (R^2=0.480, Eq. 13, Table VIII) or Log MW, DN and Log *P* (R^2=0.516, Eq. 13, Table IX) in the model. Exclusion of amphotericin B and the low and medium doses of TA from this dataset improved the coefficient values in both the cases (R^2=0.710, Fig. 1i; R^2=0.691, Fig. 2h).

Cross-Predictive Ability of the Models Developed

The best-fit equations obtained from various models of different subsets were used for predicting the vitreal half-lives of the remaining molecules in the excluded set that was not used for the model development. The coefficient of determination between the predicted and actual half-lives (Q^2) of the different best-fit models is shown in Fig. 3. Poor correlation (Q^2) was observed in the presence of amphotericin B and triamcinolone acetonide in all the predicted subsets. However, the exclusion of both these molecules from all the predicted subsets increased the predictive ability of the models. In case of Log *D* set of variables, the model obtained without salts had good predictive ability on salts as indicated by its high correlation value (Q^2=0.8007, Fig. 3). The best-fit equations obtained with pigmented set (Q^2=0.6695), acids (Q^2=0.6649) and zwitterions (Q^2=0.6687) had reasonable predictive ability on their excluded sets. In the case of Log *P* set of variables, the model obtained without salts had good predictive ability on salts as indicated by its high correlation value (Q^2=0.9043). The next best-fit equation with high predictive ability was from the albino set (Q^2=0.8137) which predicted the pigmented set of molecules with good accuracy. The other best-fit equations with reasonable predictive ability in this group were from acids (Q^2=0.5926), pigmented set (Q^2=0.5736) and zwitterions (Q^2=0.5189).

The predictive ability of the best-fit equations developed from the whole dataset using either Log *D* or Log *P* was tested on various subsets (Fig. 4). The best-fit equation developed using Log *D* had better predicting ability on the following subsets: albino (Q^2=0.8178), suspensions (Q^2=0.8765), all without suspensions (Q^2=0.7115), all without macromolecules (Q^2=0.7773), all without salts (Q^2=0.7587), acids (Q^2=0.4234) and bases (Q^2=0.8637). The best-fit equation developed using Log *P* had better predicting ability on pigmented set (Q^2=0.8146), macromolecules (Q^2=0.6770), salts (Q^2=0.9042), zwitterions (Q^2=0.7403) and neutral molecules (Q^2=0.9128).

DISCUSSION

In the present study, QSPKR based models were developed to understand the important physicochemical properties that influence the vitreal disposition of molecules in rabbit eyes. Unlike the previous models developed from a small set of molecules with structural similarity, the present data set included structurally diverse compounds with a wide range of molecular weights, lipophilicity, and solubility. The data was analyzed as a whole as well as under select classifications based on eye pigmentation, acid/base properties of the drugs, solubility, and molecular weights. Log MW, Log *P* (partition coefficient), Log *D* (distribution coefficient at pH 7), dose number (DN=Dose injected/Solubility at pH 7.4), pigmentation factor (PF) and salt factor (SF) were selected as the independent variables for regression analysis. Multiple linear regression analysis was done using two sets of variables. In the first case Log MW, Log *D*, DN, PF and SF were used as the independent variables for model development. In the second case Log *D* was replaced by Log *P* for

Table VIII. Summary of the models developed with Log MW, Log *D*, PF, SF and Dose/sol 7.4 from different groups with the best-fit equations and statistical parameters

Equation	Model[a]	Best-fit equation[b]	*N*	R^2	Adj R^2	SE	*F*	*P*
1	All	Log $t_{1/2}$=−0.156 (0.341)+0.306 (0.126) Log MW−0.083 (0.018) Log *D*+0.007 (0.001) dose/sol 7.4	63	0.512	0.487	0.427	20.59	2.9×10^{-9}
1a	All—3 outliers (amphotericin+TA low and medium dose)	Log $t_{1/2}$=−0.178 (0.221)+0.267 (0.082) Log MW−0.093 (0.012) Log *D*+0.003 (0.0004) dose/sol 7.4+0.153 (0.085) PF	60	0.725	0.705	0.275	36.29	7.8×10^{-15}
2	Albino	Log $t_{1/2}$=−0.157 (0.374)+0.295 (0.138) Log MW−0.090 (0.022) Log *D*+0.004 (0.001) dose/sol 7.4	48	0.551	0.521	0.452	18.02	8.9×10^{-8}
2a	Albino—3 outliers (amphotericin+TA low and medium dose)	Log $t_{1/2}$=−0.161 (0.197)+0.252 (0.072) Log MW−0.105 (0.011) Log *D*+0.003 (0.0003) dose/sol 7.4	45	0.820	0.806	0.236	62.09	2.7×10^{-15}
3	Pigmented	Log $t_{1/2}$=0.683 (0.170)−0.072 (0.038) Log *D*+0.047 (0.019) dose/sol 7.4	15	0.351	0.243	0.305	3.25	0.075
4	Acids	Log $t_{1/2}$=0.367 (0.122)−0.119 (0.032) Log *D*	13	0.554	0.514	0.261	13.68	0.004
5	Bases	Log $t_{1/2}$=0.60 (0.054)−0.098 (0.009) Log *D*−0.174 (0.086) dose/sol 7.4	15	0.930	0.918	0.139	79.25	1.2×10^{-7}
6	Zwitterions	Log $t_{1/2}$=−2.559 (1.37)+1.313 (0.503) Log MW	18	0.299	0.255	0.412	6.83	0.019
6a	Zwitterions—1 outlier (amphotericin)	Log $t_{1/2}$=0.554 (0.127)−0.114 (0.032) Log *D*	17	0.452	0.415	0.272	12.37	0.003
7	Neutrals	Log $t_{1/2}$=−3.230 (0.822)+1.850 (0.37) Log MW+0.002 (0.001) dose/sol 7.4	9	0.904	0.872	0.420	28.37	0.001
8	Suspensions	Log $t_{1/2}$=−10.123 (5.647)+4.361 (2.224) Log MW+0.002 (0.001) dose/sol 7.4	11	0.709	0.636	0.569	9.73	0.007
9	All without suspensions	Log $t_{1/2}$=−0.317 (0.261)+0.324 (0.095) Log MW−0.104 (0.014) Log *D*	54	0.555	0.537	0.321	31.75	1.1×10^{-9}
9a	All without suspensions—1 outlier (amphotericin)	Log $t_{1/2}$=−0.240 (0.192)+0.281 (0.07) Log MW−0.107 (0.01) Log *D*	53	0.705	0.693	0.236	59.73	5.6×10^{-14}
10	Macromolecules	Log $t_{1/2}$=−0.021 (0.307)+0.189 (0.08) Log MW+0.192 (0.123) PF+0.746 (0.11) SF	6	0.980	0.950	0.087	32.92	0.030
11	All without macromolecules	Log $t_{1/2}$=−1.069 (0.574)+0.678 (0.227) Log MW−0.072 (0.019) Log *D*+0.004 (0.001) dose/sol 7.4	57	0.541	0.515	0.429	20.84	4.7×10^{-9}
11a	All without macromolecules—3 outliers (amphotericin+TA low and medium dose)	Log $t_{1/2}$=−0.472 (0.389)+0.396 (0.155) Log MW−0.094 (0.013) Log *D*+0.003 (0.0004) dose/sol 7.4	54	0.720	0.703	0.283	42.89	7.3×10^{-14}
12	Salts	Log $t_{1/2}$=−1.613 (0.661)+0.782 (0.239) Log MW−0.112 (0.014) Log *D*	11	0.911	0.888	0.164	40.76	6.4×10^{-5}
13	All without salts	Log $t_{1/2}$=−0.073 (0.380)+0.286 (0.141) Log MW−0.073 (0.023) Log *D*+0.004 (0.001) dose/sol 7.4	52	0.480	0.447	0.461	14.76	6.1×10^{-7}
13a	All without salts—3 outliers (amphotericin+TA low and medium dose)	Log $t_{1/2}$=−0.112 (0.241)+0.244 (0.089) Log MW−0.086 (0.015) Log *D*+0.003 (0.0004) dose/sol 7.4+0.196 PF	49	0.710	0.683	0.289	26.91	2.5×10^{-11}

TA low=0.3 mg and TA medium=4 mg (both in albino)

[a] Model built with selected non-collinear independent variables using the backward stepwise multiple linear regression analysis (SPSS 11.5, SPSS Inc., IL)

[b] Values in parenthesis indicate the standard error

Table IX. Summary of the models developed with Log MW, Log *P*, PF, SF and dose/sol 7.4 from different groups with the best-fit equations and statistical parameters

Equation	Model[a]	Best-fit equation[b]	*N*	R^2	Adj R^2	SE	*F*	*P*
1	All	Log $t_{1/2}$=−0.351 (0.333)+0.465 (0.125) Log MW−0.148 (0.028) Log *P*+0.003 (0.001) dose/sol 7.4	63	0.552	0.530	0.409	24.28	2.3×10^{-10}
1a	All—3 outliers (amphotericin+TA low and medium dose)	Log $t_{1/2}$=−0.320 (0.228)+0.432 (0.086) Log MW−0.157 (0.019) Log *P*+0.003 (0.0004) dose/sol 7.4	60	0.712	0.697	0.279	46.25	3.6×10^{-15}
2	Albino	Log $t_{1/2}$=−0.316 (0.381)+0.450 (0.144) Log MW−0.147 (0.035) Log *P*+0.003 (0.001) dose/sol 7.4	48	0.553	0.522	0.451	18.11	8.4×10^{-8}
2a	Albino—3 outliers (amphotericin+TA low and medium dose)	Log $t_{1/2}$=−0.286 (0.241)+0.409 (0.091) Log MW−0.150 (0.022) Log *P*+0.003 (0.0004) dose/sol 7.4	45	0.738	0.718	0.285	38.41	5.5×10^{-12}
3	Pigmented	Log $t_{1/2}$=−1.055 (0.477)+0.7 (0.179) Log MW−0.199 (0.03) Log *P*+0.049 (0.009) dose/sol 7.4	15	0.852	0.811	0.152	21.03	7.3×10^{-5}
4	Acids	Log $t_{1/2}$=0.841 (0.09)−0.150 (0.051) Log *P*	13	0.435	0.384	0.294	8.48	0.014
5	Bases	Log $t_{1/2}$=0.811 (0.056)−0.191 (0.02) Log *P*+0.203 (0.099) SF	15	0.888	0.869	0.176	47.35	2.0×10^{-6}
6	Zwitterions	Log $t_{1/2}$=−2.559 (1.37)+1.313 (0.503) Log MW	18	0.299	0.255	0.412	6.83	0.019
6a	Zwitterions—1 outlier (amphotericin)	Log $t_{1/2}$=0.806 (0.05)−0.169 (0.028) Log *P*+0.257 (0.118) SF	17	0.766	0.733	0.184	22.92	3.8×10^{-5}
7	Neutrals	Log $t_{1/2}$=−3.230 (0.822)+1.850 (0.37) Log MW+0.002 (0.001) dose/sol 7.4	9	0.904	0.872	0.420	28.37	0.001
8	Suspensions	Log $t_{1/2}$=−22.348 (6.648)+9.255 (2.642) Log MW−0.376 (0.153) Log *P*+0.002 (0.001) dose/sol 7.4	11	0.844	0.777	0.445	12.61	0.003
9	All without suspensions	Log $t_{1/2}$=−0.424 (0.277)+0.477 (0.104) Log MW−0.158 (0.023) Log *P*	54	0.513	0.494	0.336	26.83	1.1×10^{-8}
9a	All without suspensions—1 outlier (amphotericin)	Log $t_{1/2}$=−0.350 (0.213)+0.438 (0.08) Log MW−0.162 (0.018) Log *P*	53	0.646	0.632	0.258	45.59	5.4×10^{-12}
10	Macromolecules	Log $t_{1/2}$=−0.021 (0.307)+0.189 (0.08) Log MW+0.192 (0.123) PF+0.746 (0.11) SF	6	0.980	0.950	0.087	32.92	0.030
11	All without macromolecules	Log $t_{1/2}$=−1.448 (0.54)+0.903 (0.212) Log MW−0.137 (0.029) Log *P*+0.003 (0.001) dose/sol 7.4	57	0.593	0.570	0.404	25.79	2.0×10^{-10}
11a	All without macromolecules—3 outliers (amphotericin+TA low and medium dose)	Log $t_{1/2}$=−0.961 (0.38)+0.687 (0.149) Log MW−0.148 (0.02) Log *P*+0.003 (0.0004) dose/sol 7.4	54	0.731	0.714	0.278	45.18	2.9×10^{-14}
12	Salts	Log $t_{1/2}$=1.012 (0.05)−0.211 (0.022) Log *P*	11	0.909	0.898	0.156	89.51	5.7×10^{-6}
13	All without salts	Log $t_{1/2}$=−0.302 (0.379)+0.443 (0.144) Log MW−0.135 (0.035) Log *P*+0.003 (0.001) dose/sol 7.4	52	0.516	0.486	0.445	17.04	1.1×10^{-7}
13a	All without salts—3 outliers (amphotericin+TA low and medium dose)	Log $t_{1/2}$=−0.268 (0.253)+0.403 (0.096) Log MW−0.147 (0.023) Log *P*+0.003 (0.0004) dose/sol 7.4	49	0.691	0.670	0.296	33.48	1.5×10^{-11}

TA low=0.3 mg and TA medium=4 mg (both in albino)

[a] Model built with selected non-collinear independent variables using the backward stepwise multiple linear regression analysis (SPSS 11.5, SPSS Inc., IL)

[b] Values in parenthesis indicate the standard error

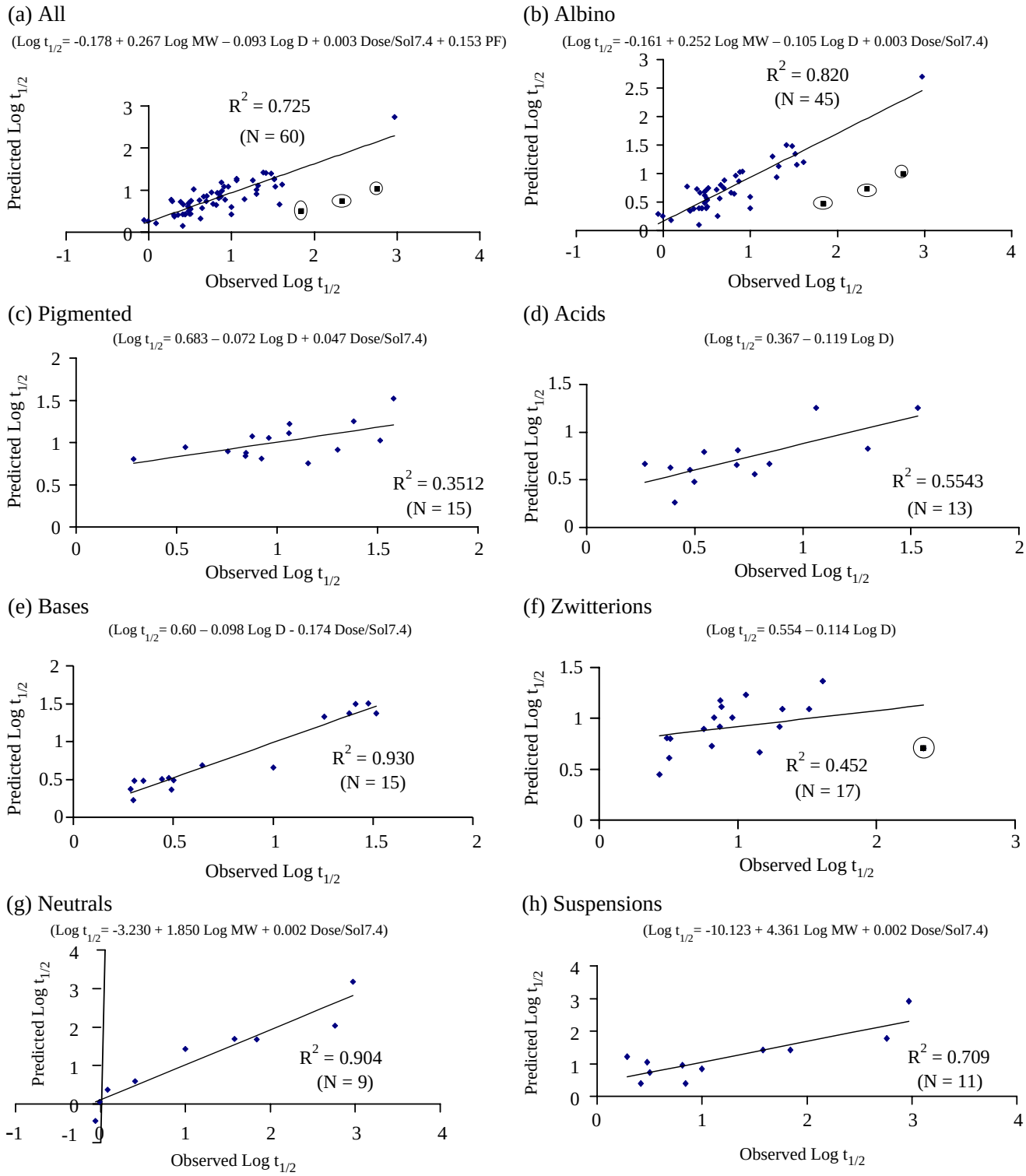

Fig. 1. Scatterplots of the best-fit models developed using Log *D* set of variables along with the best-fit equation for entire dataset (**a**), and various subsets including albino (**b**), pigmented (**c**), acids (**d**), bases (**e**), zwitterions (**f**), neutrals (**g**), suspensions (**h**), all without suspensions (**i**), macromolecules (**j**), all without macromolecules (**k**), salts (**l**), all without salts (**m**). The excluded outliers are shown in the *circles*.

(i) All without suspension

(Log t1/2= -0.240 + 0.281 Log MW –0.107 Log D)

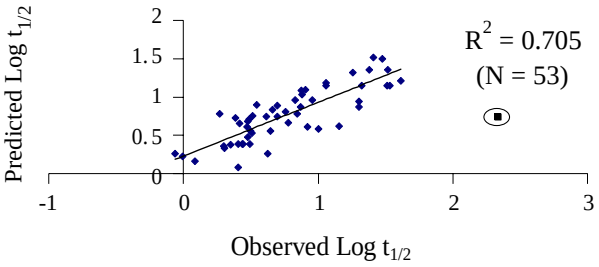

(j) Macromolecules

(Log $t_{1/2}$ = -0.021 + 0.189 Log MW + 0.192 PF + 0.746 SF)

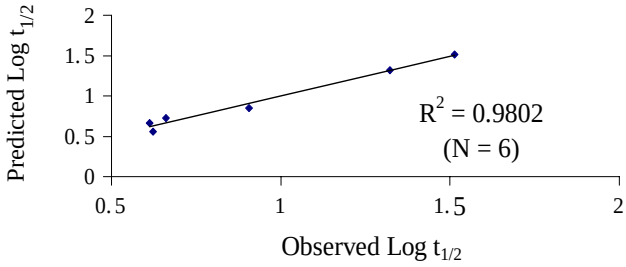

(k) All without macromolecules

(Log $t_{1/2}$ = -0.472 + 0.396 Log MW – 0.094 Log D + 0.003 Dose/Sol7.4)

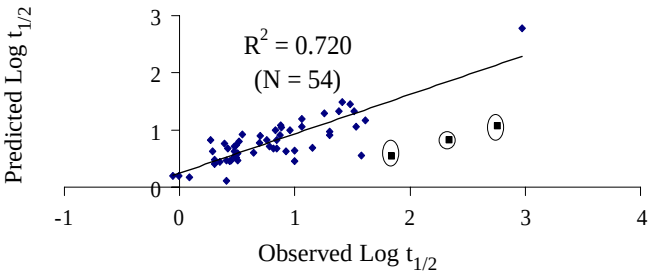

(l) Salts

(Log $t_{1/2}$ = -1.613 + 0.782 Log MW – 0.112 Log D)

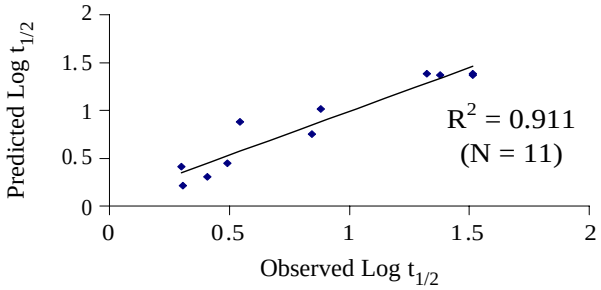

(m) All without salts

(Log $t_{1/2}$ = -0.112 + 0.244 Log MW – 0.086 Log D + 0.003 Dose/Sol7.4 + 0.196 PF)

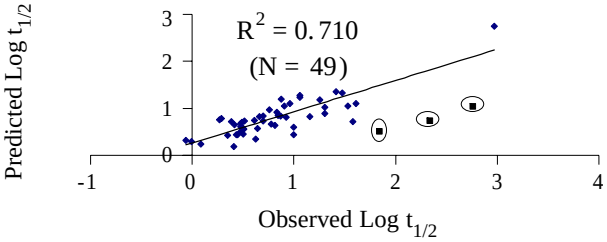

Fig. 1. (continued).

model development. Although both Log *D* (distribution coefficient) and Log *P* (partition coefficient) denote the lipophilicity of a molecule, Log *D* takes into account the ionization of compounds at different pH values. Hence regression analysis was performed using both these variables to better understand their influence on molecular properties. The selected independent variables were checked for multicollinearity (condition that exists when two or more independent variables are related to each other leading to unreliable estimation of regression coefficients) and the best-fit models were obtained for the entire dataset and different subsets. The best-fit models developed indicated that Log MW, Log *D* or Log *P* and dose number (DN=dose/solubility at pH 7.4) as the important noncollinear variables that best describe the vitreal disposition of molecules in various sets.

Multiple linear regression analysis of the selected noncollinear variables was found to be highly correlated with K_{10} half-lives of both one and two compartments rather than the beta half-lives. In case of one compartment pharmacokinetic model, the elimination half-life of the drug from the injected compartment (vitreous) is represented only by the K_{10} half-life. However, from a two compartment model (which includes a distribution compartment) alpha, beta and K_{10} half-lives can be estimated. The alpha half-life represents the distribution phase and the beta half-life denotes the elimination phase. The K_{10} half-life reflects the elimination of drug from the injected compartment (central compartment) and is derived from the relation (alpha×beta)/K_{21}. In this study, inclusion of K_{10} half-lives resulted in good correlations with the predictor variables.

Exclusion of amphotericin and triamcinolone acetonide (TA, low and medium doses) from the entire dataset and other subsets (except suspensions) resulted in models with high correlation value (R^2) and statistically significant coefficients for the independent variables. However, TA high dose (16 mg) was well fit in the models developed. In

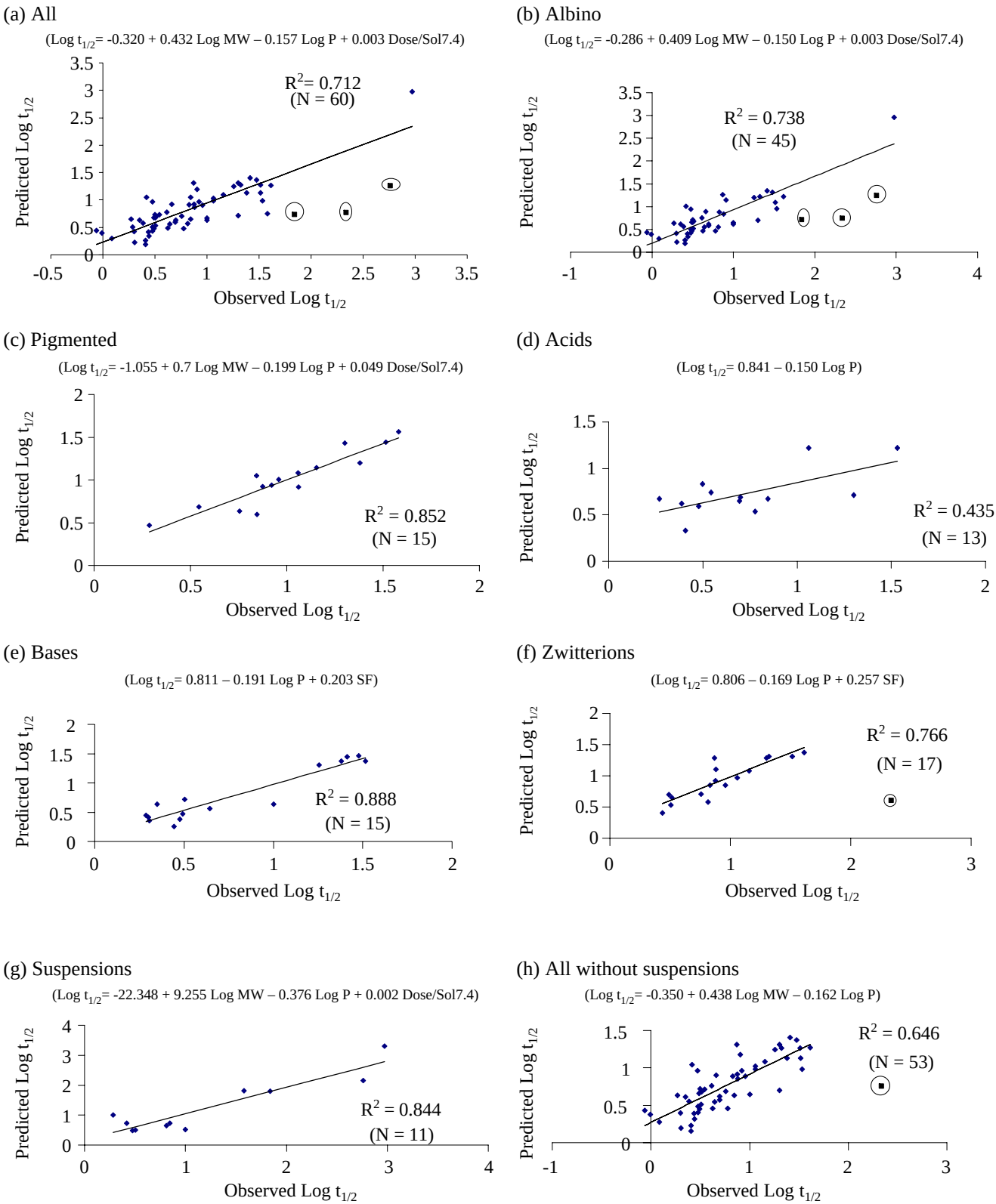

Fig. 2. Scatterplots of the best-fit models developed using Log *P* set of variables along with the best-fit equation for entire dataset (**a**), and various subsets including albino (**b**), pigmented (**c**), acids (**d**), bases (**e**), zwitterions (**f**), suspensions (**g**), all without suspensions (**h**), all without macromolecules (**i**), salts (**j**), all without salts (**k**). The excluded outliers are shown in the *circles*. The best-fit equation obtained for macromolecules and neutral compounds is the same as mentioned in the Log *D* set of variables.

(i) All without macromolecules

(Log $t_{1/2}$= -0.961 + 0.687 Log MW – 0.148 Log P + 0.003 Dose/Sol7.4)

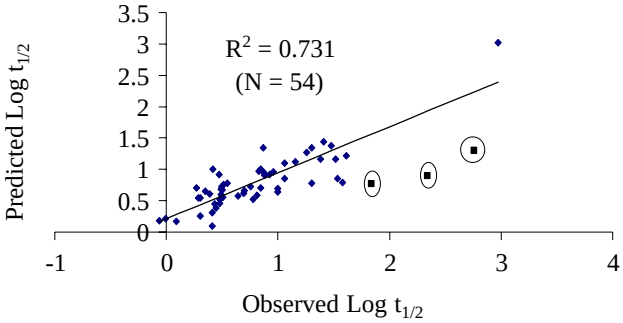

(j) Salts

(Log $t_{1/2}$= 1.012 – 0.211 Log P)

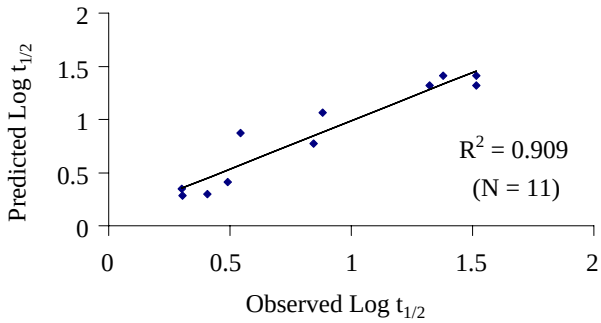

(k) All without salts

(Log $t_{1/2}$= -0.268 + 0.403 Log MW –0.147 Log P + 0.003 Dose/Sol7.4)

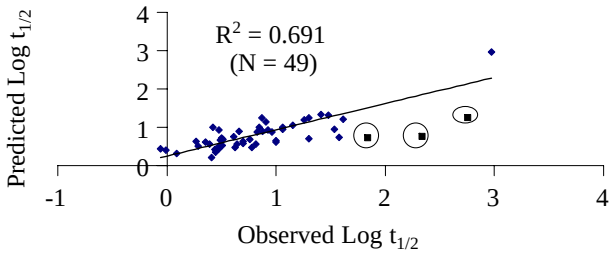

Fig. 2. (continued).

the two studies reporting the intravitreal clearance of amphotericin B (29,30), the time points included for half-life estimation were taken on days 1, 3, 6, 9, 12 or on days 1, 5, 10, and 15. Thus, insufficient time points were taken during the first 24 h, indicating that the half-life calculated with these points could be of the beta phase. Similar was the case with triamcinolone acetonide where time points were days 1, 2, 4, 7, 12, 20, and 30 in albino rabbits (TA low dose, 0.3 mg) (31), 1, 7, 14, 28, 42, 56, and 120 days (TA medium dose, 4 mg) in another study with albino rabbits (61), and days 1, 2, 3, 6, 13, 21, and 46 in pigmented rabbits (32). When sufficient time points were not included in pharmacokinetic studies, the results might under- or over-estimate some of the important pharmacokinetic parameters. Hence, these two drugs were excluded and stepwise regression analysis was performed

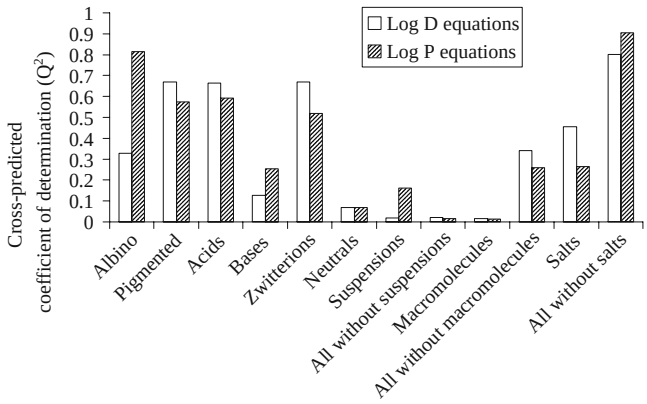

Fig. 3. Cross-predictive ability of the models developed from different subsets on rest of molecules in the excluded set that was not used for the model development.

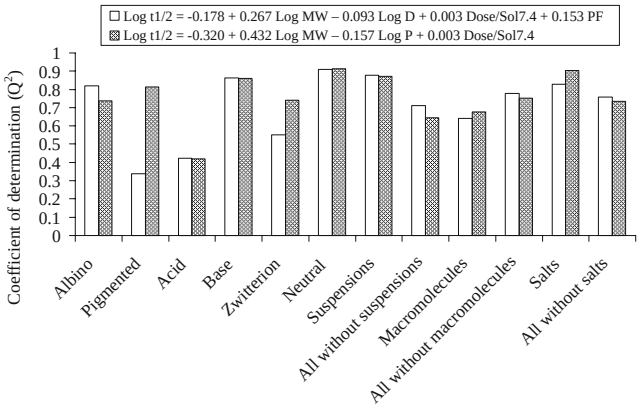

Fig. 4. Predictive ability of the best-fit equations obtained with entire dataset on various subsets. The best-fit equation obtained using Log *D* from the whole dataset without outliers (Log $t_{1/2}$=−0.178+0.267 Log MW−0.093 Log *D*+0.003 dose/sol 7.4+0.153 PF) predicted the following subsets: albino, suspensions, all without suspensions, all without macromolecules, all without salts, acids, and bases with high correlation values. The best-fit equation obtained using Log *P* from the whole dataset without outliers (Log $t_{1/2}$=−0.320+0.432 Log MW −0.157 Log *P*+0.003 dose/sol 7.4) predicted the following subsets: pigmented, macromolecules, salts, zwitterions, and neutral molecules with high correlation values and less residual errors.

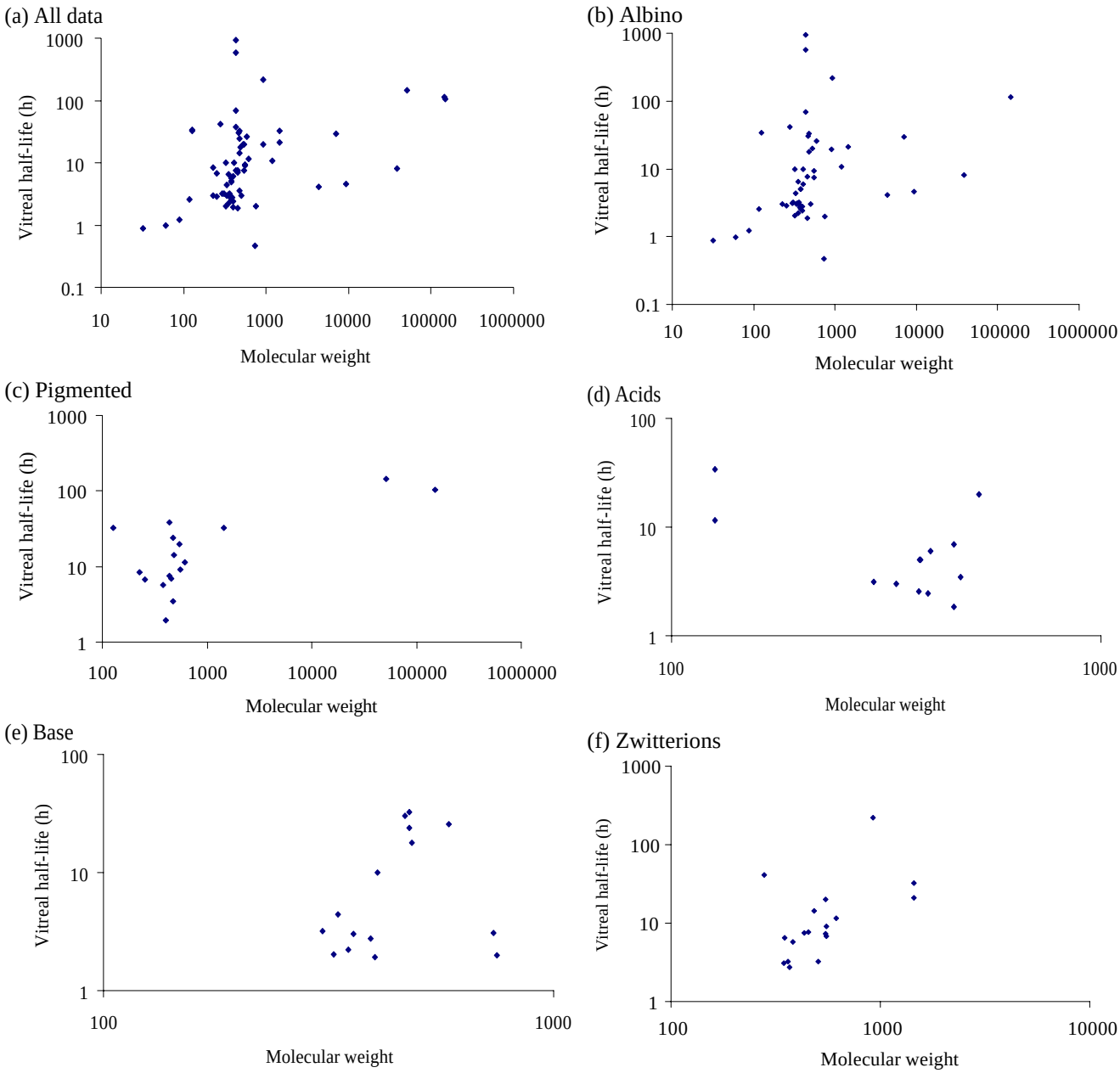

Fig. 5. Plot of vitreal half-life as a function of molecular weight for entire dataset (**a**), albino group (**b**), pigmented group (**c**), acids (**d**), bases (**e**), zwitterions (**f**), neutrals (**g**), suspensions (**h**), and macromolecules (**i**). Both vitreal half-life and molecular weight are shown in logarithmic scale.

without them to determine the variables that most influence the vitreal half-life.

The best-fit equations developed after excluding amphotericin B and TA (low and medium doses) from the entire dataset included all three important variables, namely, Log MW, Log *P* or Log *D* and DN. After exclusion of the outliers, the R^2 values increased significantly (>0.7), justifying their omission. The equation obtained with Log *D* set of variables included pigmentation factor as an additional variable when compared with Log *P* set of variables. These equations predicted the different subsets with good accuracy (Q^2>0.71) except acids (Q^2=0.4234) and macromolecules (Q^2=0.6770) as shown in Fig. 4. The predictive abilities of both these equations improved after excluding amphotericin B, and triamcinolone acetonide (low and medium doses) from the predicted datasets. Although both the equations developed with either Log *D* or Log *P* had similar predictive abilities (not much difference in the Q^2 values), the influence of Log *P* was more pronounced in case of pigmented set and zwitterions (Fig. 4). Both these subsets were well predicted using the best-fit equation employing Log *P*.

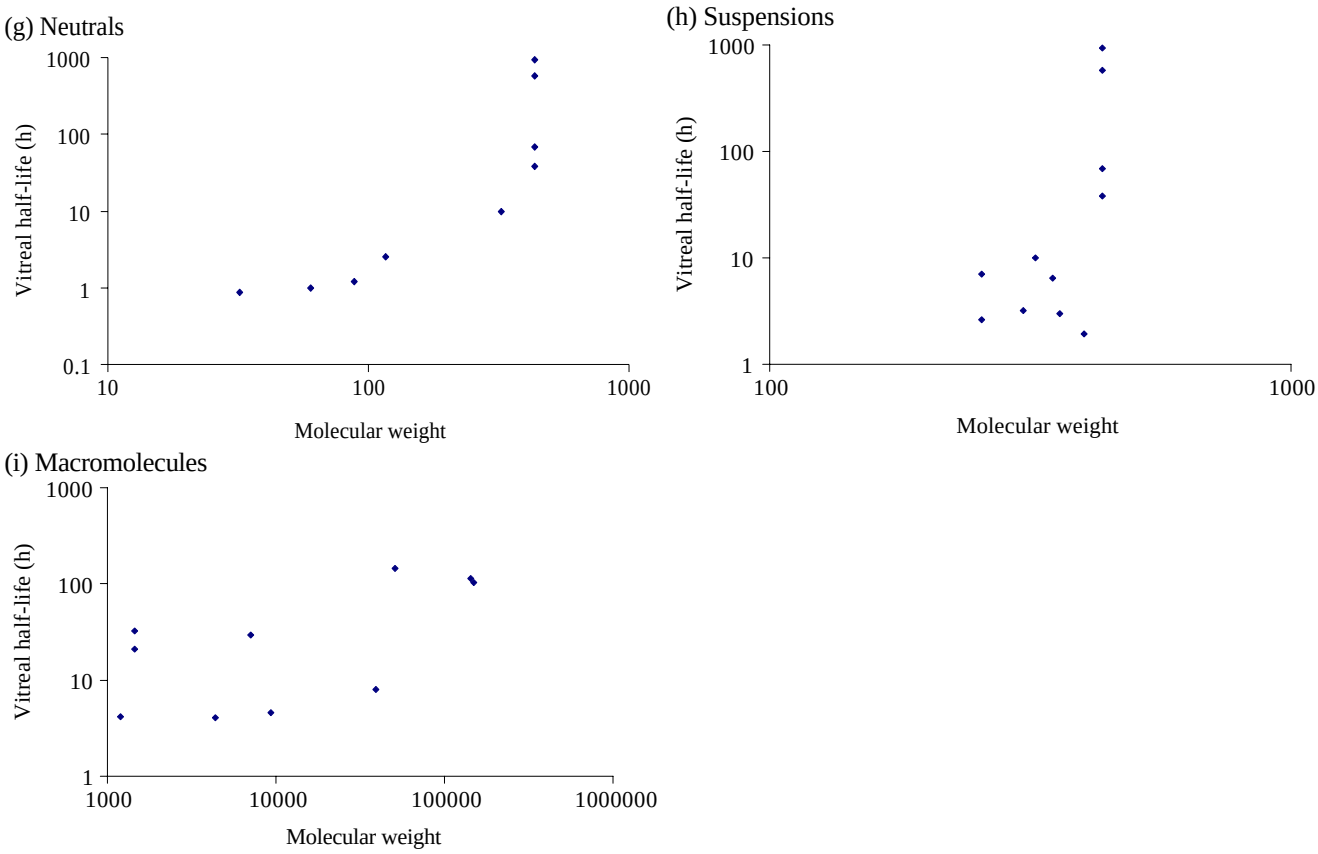

Fig. 5. (continued).

Log MW positively correlated with vitreal half-life of molecules. An increasing trend in the vitreal half-life was observed for molecules with increasing MW as seen in Fig. 5 except for the subsets acids (Fig. 5d), bases (Fig. 5e) and zwitterions (Fig. 5f). MW is an important physicochemical parameter that is known to influence the permeability of the molecule across different layers including sclera (33) and RPE (17). Similar results were reported earlier indicating an increased vitreal half-life for high MW compounds. Maurice (28) had shown that high MW compounds were eliminated from the vitreous slowly (high half-life) through the aqueous humor pathway. Also other investigators had shown the dependence of vitreal elimination on Log MW (27). However, the results obtained in this study indicate that Log MW alone does not influence the vitreal clearance of molecules tested. This was further confirmed by the poor predictive ability (Q^2=0.0977) of the previously reported equation involving only Log MW (Elimination rate constant K= 8.3767−1.5017×Log MW (27)) when applied to the entire dataset of this study (excluding amphotericin B, TA and FITC–dextrans) and only to macromolecules including FITC–dextrans (Q^2=0.0886). The increased vitreal half-life (slow clearance) could also be attributed to the slow diffusion of high MW compounds in the vitreous. Exclusion of this variable from the best-fit equations resulted in poor R^2 values (Eqs. 3, 4, 6 in Table VIII; Eq. 4 in Table IX) or poor predictive ability (less Q^2 values as shown in Fig. 3).

Log *D* and Log *P* correlated negatively with vitreal half-life, indicating shorter half-life for highly lipophilic molecules. This trend is clearly indicated in the scatter plots shown in Figs. 6 and 7. The decreasing trend is observed for the entire dataset and various subsets except neutral molecules (Figs. 6g and 7g), macromolecules (Figs. 6i and 7i), and suspensions (Fig. 7h). Intravitreally administered molecules are eliminated from the vitreous by either anterior (aqueous humor) or posterior (retina) route (28). Molecules eliminated by the anterior route diffuse into the anterior chamber and are excreted through the canal of Schlemm. Due to this long route and relatively less effective area of elimination pathway, molecules eliminated by this route have a long vitreal half-life and it is hypothesized as the major route of elimination for hydrophilic molecules. Retinal route is the major elimination pathway for lipophilic drugs. Because of the large surface area, tissue partitioning as well as active transport mechanisms, the vitreal half-life of molecules eliminated by this route is usually short. Thus, lipophilicity of a molecule determines its elimination pathway from the vitreous and thereby influences the vitreal half-life. Liu *et al.* (26) had previously reported a linear correlation between the lipophilicity (Log *D* at pH 7.2) and beta half-life using a small group (four) of structurally similar quinolones. How-

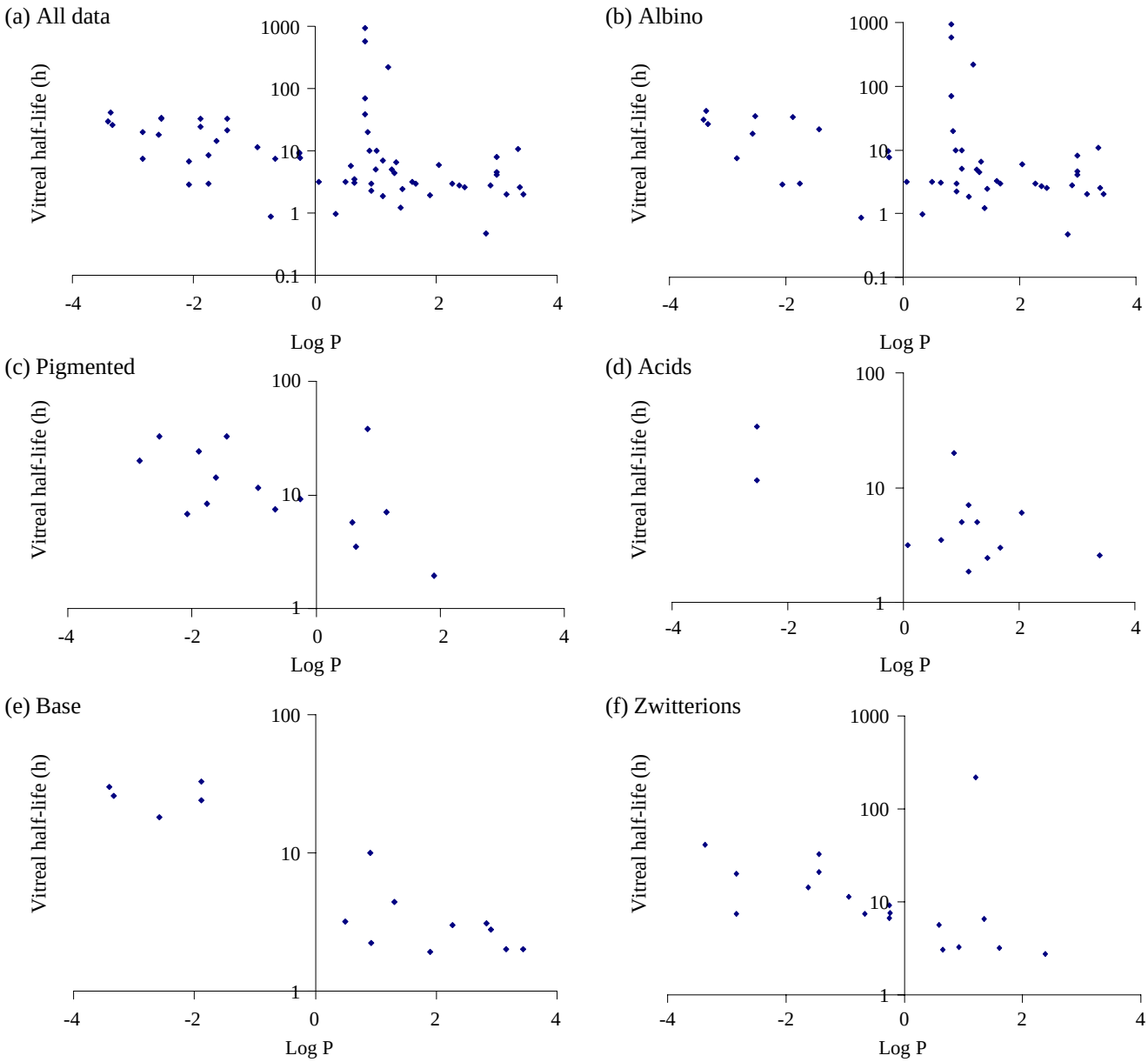

Fig. 6. Plot of vitreal half-life as a function of Log *P* for entire dataset (**a**), albino group (**b**), pigmented group (**c**), acids (**d**), bases (**e**), zwitterions (**f**), neutrals (**g**), suspensions (**h**), and macromolecules (**i**). Vitreal half-life is shown in logarithmic scale.

ever, the predictive ability of the equation ($t_{1/2,\beta}$=−1.8172× Log $D_{\text{pH 7.2}}$+2.1239) when applied to the dataset of the current study (excluding amphotericin B, triamcinolone acetonide, and the four quinolones used by the authors to develop the model) was low with a Q^2 of 0.1217. Also the best fit models obtained in this study involving only Log *D* (Eqs. 4 and 6 in Table VIII) or only Log *P* (Eqs. 4 and 12 in Table IX) exhibited poor predictive ability (less Q^2 values, Fig. 3). All these results clearly indicate that lipophilicity alone is not useful as a predictor of vitreal half-life of diverse compounds.

Dose number (DN=dose/solubility at pH 7.4) is an important variable in the models developed. DN positively correlated with vitreal half-life of molecules (Fig. 8). During the initial regression analysis of the dataset where dose was not included as a variable, the models developed had R^2 values in the range of 0.348 (suspensions) to 0.918 (macromolecules) and no best-fit model could be obtained for suspensions. Inclusion of DN, which accounts for the dose administered and the solubility of the molecule, improved the best-fit models and resulted in high R^2 values and good predictive ability. Addition of DN resulted in highly significant best-fit model for all suspensions (R^2=0.844, Fig. 2d) which could account for different doses of TA administered. When the dose injected exceeds the solubility of a molecule, a declining fraction of the injected dose gets absorbed and/or cleared, resulting in dose-dependent pharmacokinetics or half-life for suspensions.

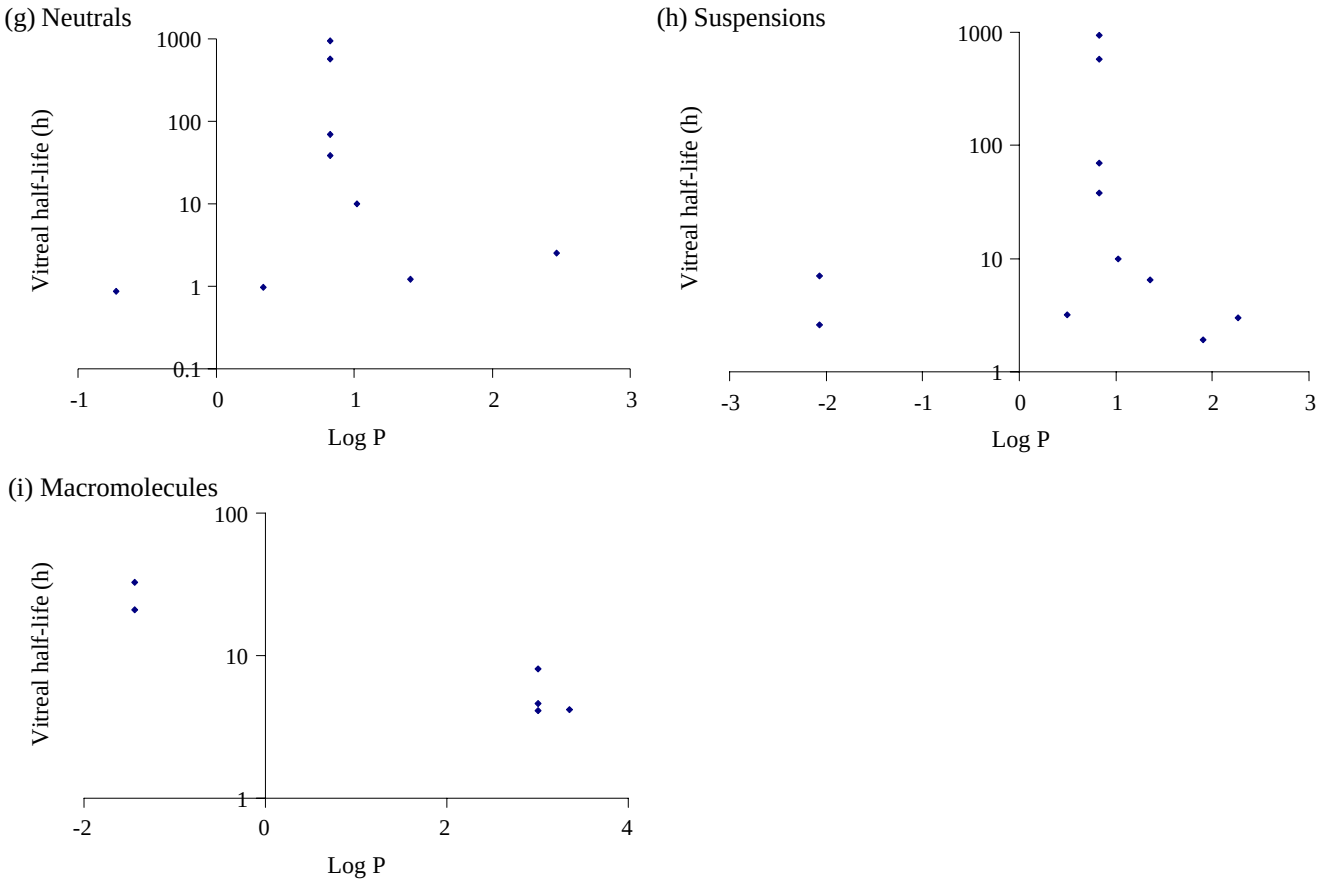

Fig. 6. (continued).

The best-fit model generated with the data obtained from albino rabbits indicated that three parameters (Log MW, Log *D* or Log *P* and DN) were important in predicting the vitreal half-life of molecules (R^2=0.820, Fig. 1b; R^2=0.738, Fig. 2b). However, the best-fit equation involving Log *P* predicted the pigmented data with high accuracy (Q^2=0.8137, Fig. 3). Another interesting observation in this analysis was the role of Log *P* in pigmented groups. No significant model could be obtained in the pigmented group when Log *D* was used as the independent variable (Table VIII, Eq. 3, R^2=0.351). Also, the predictive ability of albino group equation developed using Log *D* was very poor on the pigmented set (Q^2= 0.3271, Fig. 3). However, when Log *P* was used, a model with high correlation coefficient could be developed for the pigmented set (R^2=0.852, Fig. 2c). This was further supported by the high predictive ability of the albino set equation developed with Log *P* on the pigmented set (Q^2=0.8137, Fig. 3). These observations clearly indicate that Log *P* (not Log *D*) is an important variable that influences the pharmacokinetic properties of molecules in pigmented animals.

None of the models obtained from acids, bases, and zwitterions had Log MW in their best-fit equations (Tables VIII and IX). Lipophilicity turned out to be the important variable that influences the vitreal half-life of these molecules. These molecules get ionized at physiological pH at the injected site (vitreous) and hence changes occur in their solubility and lipophilicity (ionized molecules were more water soluble than the nonionized form). Hence the best-fit models developed from these ionizable molecules included either Log *D* or Log *P* in the best-fit equations. The best-fit model obtained for acids included only Log *D* (Fig. 1j) or Log *P* (Fig. 1i) in the equation and had poor R^2 and Q^2 values (Fig. 3). In case of bases, the molecules were best-fit using both Log *D* and DN or Log *P* (R^2>0.88). In case of zwitterions, Log *P* resulted in better-fit model (R^2=0.766, Fig. 2k) when compared with Log *D*. This could be a result of the difficulty in estimation of Log *D* values for zwitterions due to their multiple charges. In case of neutral molecules, the best-fit model was obtained with Log MW and DN. Since neutral molecules exhibit neutral charge at physiological pH, the vitreal half-life of these molecules was influenced by Log MW rather than lipophilicity. Although these models had high R^2 (>0.76 except acids), their predictive abilities were poor. All these data further strengthen the fact that all three predictor variables (Log MW, Log *D* or Log *P* and DN) are essential for predicting the vitreal disposition of molecules.

The advantage of including DN as a variable was obvious from the best-fit model obtained for suspensions. Without inclusion of DN, no best-fit models could be obtained for this group. The inclusion of DN along with

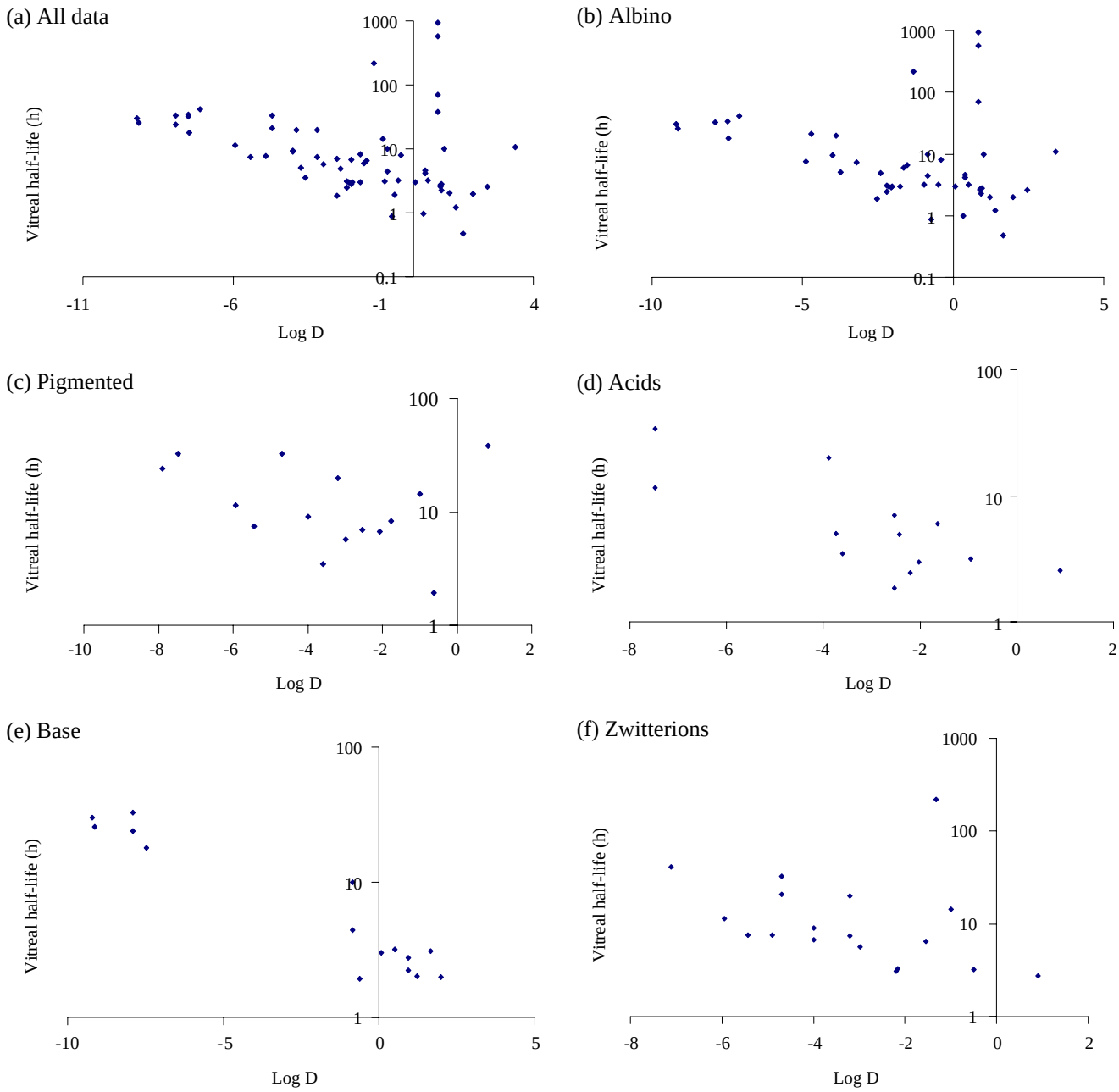

Fig. 7. Plot of vitreal half-life as a function of Log *D* for entire dataset (**a**), albino group (**b**), pigmented group (**c**), acids (**d**), bases (**e**), zwitterions (**f**), neutrals (**g**), suspensions (**h**), and macromolecules (**i**). Vitreal half-life is shown in logarithmic scale.

Log MW and Log *P* improved the fit of this group (R^2= 0.844, Eq. 8, Table IX) and also accounted for different doses of TA which was otherwise a clear outlier in other groups. Freely soluble compounds diffuse well in the vitreous and reach retina or aqueous humor and get eliminated based on their molecular properties. In case of suspensions where a high dose exceeding the solubility of molecule was injected, the dissolution of drug from the administered dosage form (suspension) becomes a crucial factor. This was further supported by a recent report by Amrite and Kompella (34), where inclusion of a dissolution–release step improved the model fits for suspensions after periocular injection. The model developed from the dataset excluding suspensions (Eq. 9, Tables VIII and IX) included only Log MW and Log *D* or Log *P*. However, the predictive ability of this equation which did not include DN was very poor (Q^2=0.0209, Fig. 3) indicating the importance of all three variables in predicting the vitreal half-life of molecules.

In case of macromolecules, the best-fit model obtained included only Log MW in the equation (Eq. 10, Tables VIII and IX). Only small molecules can freely diffuse in vitreous. Large MW molecules have decreased diffusivity and hence were slowly excreted from the vitreous. Hence in case of

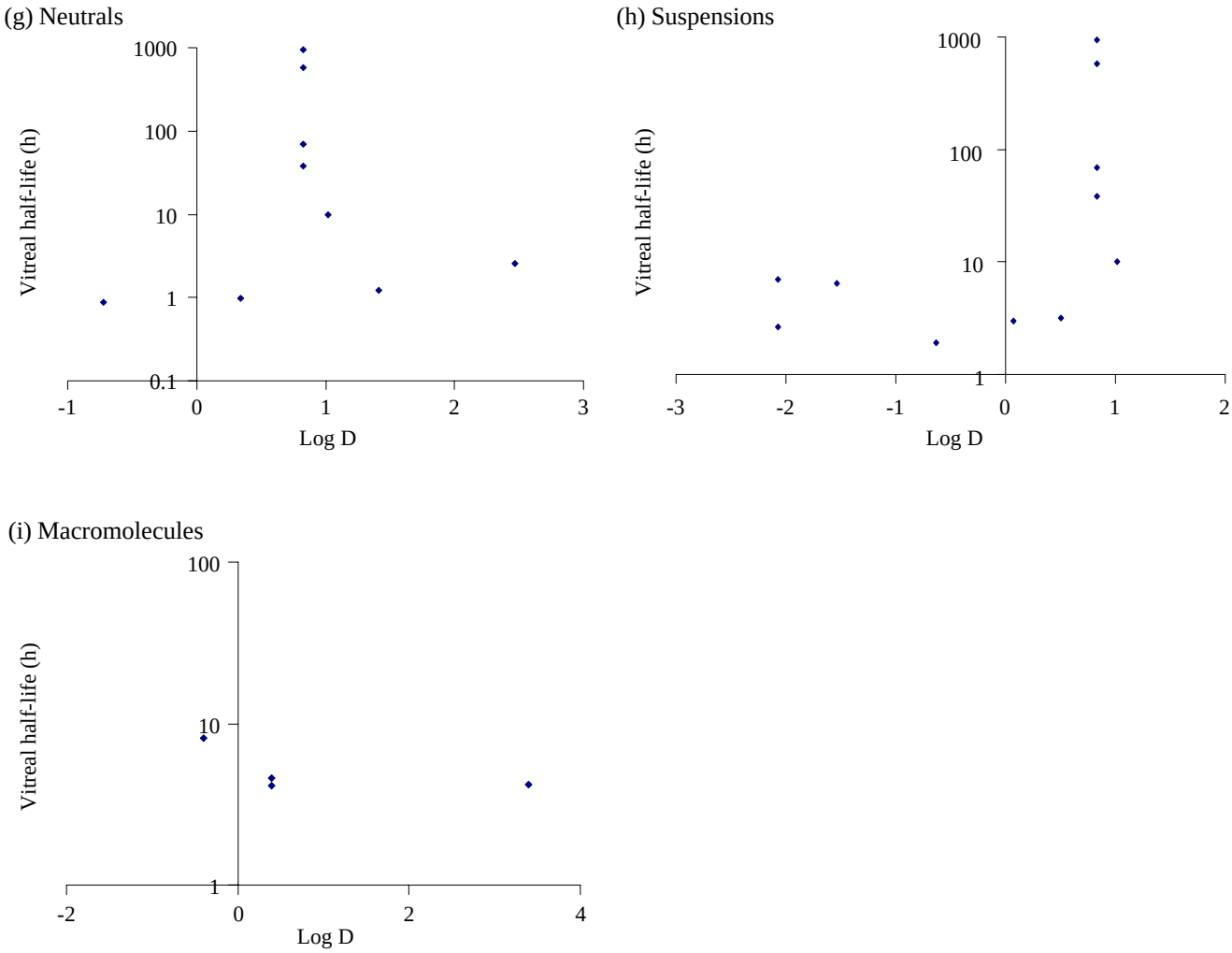

Fig. 7. (continued).

macromolecules, rather than lipophilicity and dose administered, the MW of the macromolecule influences the vitreal half-life. Though this model had the highest R^2 (0.980, Fig. 1f), its predictive ability on smaller molecules was less (Q^2=0.0155, Fig. 3). When macromolecules were excluded from the whole dataset, the best-fit equations obtained included all three variables (Eq. 11, Tables VIII and IX) showing the dependence of small molecules on lipophilicity and DN in addition to MW.

The best-fit model obtained with salts indicated Log MW and Log *D* or only Log *P* as the influential variables. Molecules in the salt form were formulated to overcome the solubility related issues during administration. Depending on the p*K*a values of the parent moiety, the salt form could have similar or altered partition/distribution coefficients after injection. Thus the best-fit models indicated the lipophilicity parameters as the important variable. The classification of salt forms in the present dataset was based on the identification of salt form by the source literature. However, in other literature reports, the exact salt form administered was not mentioned. Hence this classification should be interpreted with caution. Finally, exclusion of molecules administered as salts from the entire dataset included all three parameters and also had good predictive ability on the salt forms (Q^2=0.9043, Fig. 3) and on the experimental data.

Although drug concentration in the vitreous can be predicted based on drug physicochemical properties, drug levels in target macula region and drug persistence at the target are critical determinants of drug effects in posterior segment diseases such as AMD. However, with the present data it would be difficult to predict the drug distribution at such target sites. The data provided in the current study was an initial attempt to understand the influence of physicochemical properties on the vitreal half-life of molecules. In future, such an analysis can be potentially extended to target tissues such as the macula.

In conclusion, best-fit models were developed to predict the half-life of molecules in the vitreous after intravitreal injection. Unlike the previous reports, the present study indicates that no single parameter predicts the vitreal half-life of a diverse class of molecules. The best-fit models obtained clearly indicated Log MW, Log *D* or Log *P* and DN (dose/solubility at pH 7.4) as the critical physicochemical parameters that most influence the vitreal half-life of molecules. The best-fit model obtained in the

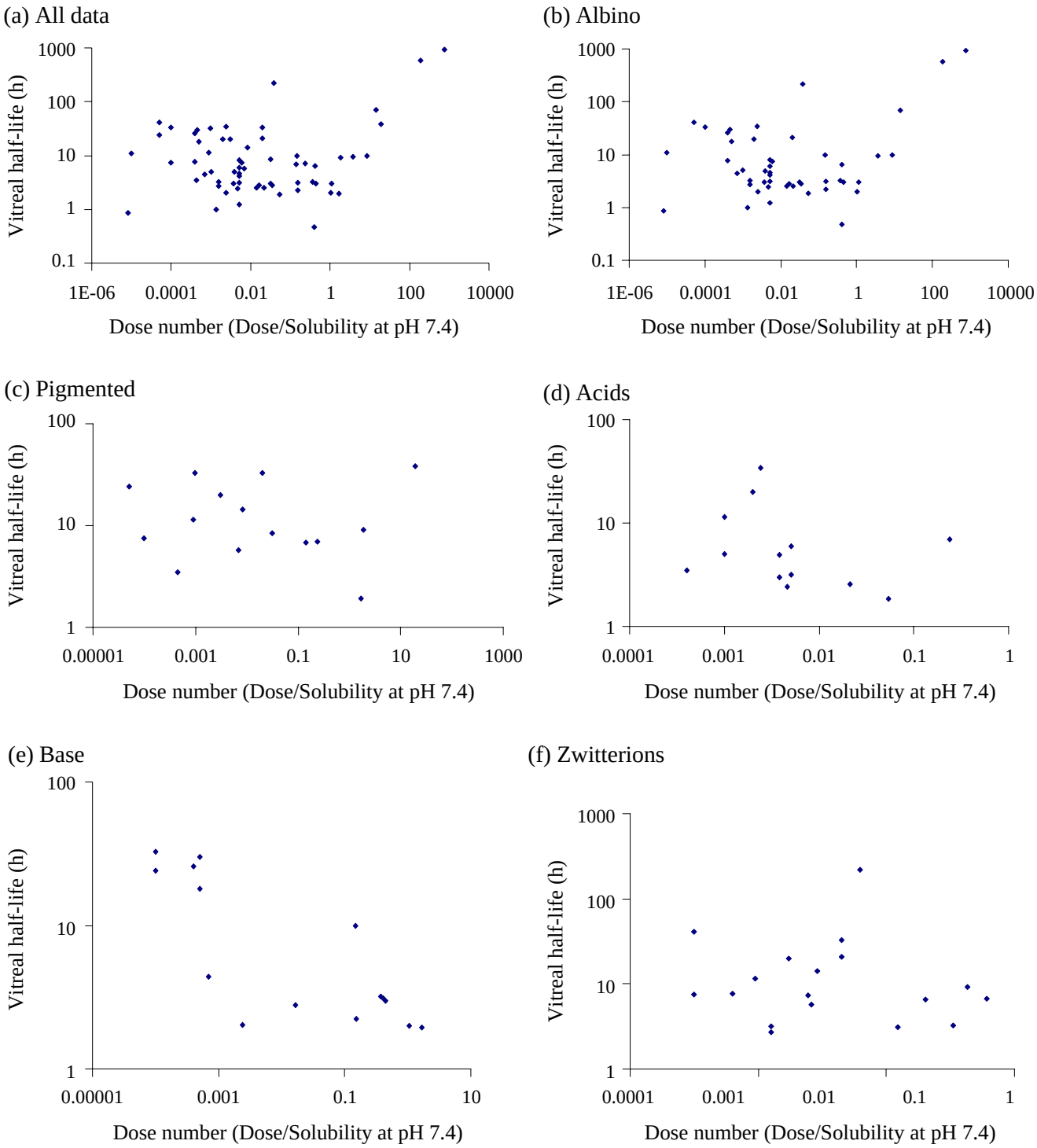

Fig. 8. Plot of vitreal half-life as a function of dose number (dose/solubility at pH 7.4) for entire dataset (**a**), albino group (**b**), pigmented group (**c**), acids (**d**), bases (**e**), zwitterions (**f**), neutrals (**g**), suspensions (**h**), and macromolecules (**i**). Both vitreal half-life and dose number are shown in logarithmic scale.

present study from the entire dataset could be used to predict the vitreal half-life of diverse group of molecules. Half-lives for the subsets bases, suspensions, non-suspensions, non-macromolecules, non-salts, and albino rabbits could be best predicted using the general equation, Log $t_{1/2}$=−0.178+0.267 Log MW−0.093 Log D+0.003 dose/solubility at pH 7.4+0.153 PF, with R^2 >0.7. Half-lives for the subsets zwitterions, neutrals, macromolecules, salts, and pigmented rabbits could be best predicted using the general equation, Log $t_{1/2}$=−0.320+0.432 Log MW−0.157 Log P+0.003 dose/solubility at pH 7.4, with

(g) Neutrals

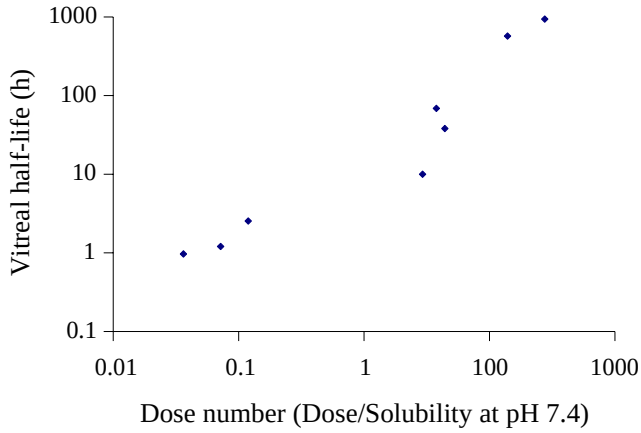

(h) Suspensions

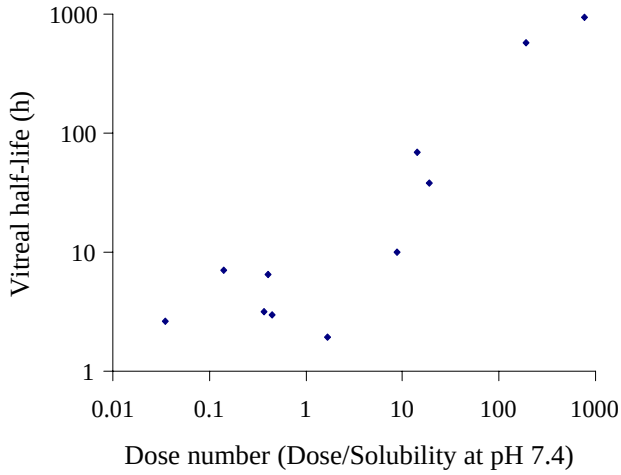

(i) Macromolecules

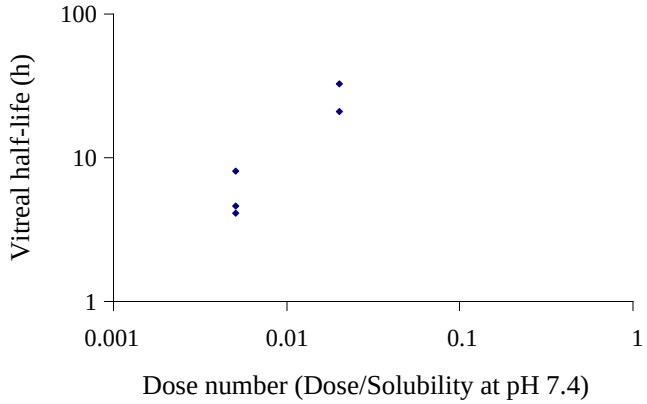

Fig. 8. (continued).

R^2>0.7. Since a large number of molecules were used in arriving at the two general equations mentioned above, these are likely to be more universal and reliable in predicting vitreal half-lives compared to other equations developed with smaller datasets. However, the smaller datasets, when expanded in future, might provide more unique and simpler equations for various subsets. The models developed for subsets of compounds provide some interesting insights. For instance, while the best-fit models for individual groups of acids, bases and zwitterions involve Log *D* or Log *P*, the best-fit model for macromolecules includes Log MW and not Log *D* or Log *P*, suggesting the importance of MW over lipophilicity in this group. To the best of our knowledge, the general model developed in the current study with the entire dataset was the first of its kind, providing a universal single model that could be used to predict the vitreal half-life of structurally diverse molecules. The best-fit models developed and approach followed in the present study will benefit not only the discovery scientists but also the clinicians in selecting the proper drug or drug form for prolonged therapy.

ACKNOWLEDGEMENTS

This work was supported by a grant from Pfizer Global Research and Development, Groton, CT, USA. The authors acknowledge Dr. Jane Meza (Biostatistics department of UNMC) for her critical review of the manuscript.

REFERENCES

1. P. M. Hughes, O. Olejnik, J. E. Chang-Lin, and C. G. Wilson. Topical and systemic drug delivery to the posterior segments. *Adv. Drug Deliv. Rev.* **57**:2010–2032 (2005). doi:10.1016/j.addr.2005.09.004.
2. D. H. Geroski, and H. F. Edelhauser. Drug delivery for posterior segment eye disease. *Invest. Ophthalmol. Vis. Sci.* **41**:961–964 (2000).
3. V. H. L. Lee, and K.-I. Hosoya. Retina. In C. P. Wilkinson (ed.), *Drug Delivery to the Posterior Segment. Vol. 3*, C.V. Mosby, Los Angeles, 2001.
4. M. D. de Smet, C. J. Meenken, and G. J. van den Horn. Fomivirsen—a phosphorothioate oligonucleotide for the treat-

ment of CMV retinitis. *Ocul. Immunol. Inflamm.* **7**:189–198 (1999). doi:10.1076/ocii.7.3.189.4007.
5. R. M. Dafer, M. Schneck, T. R. Friberg, and W. M. Jay. Intravitreal ranibizumab and bevacizumab: a review of risk. *Semin. Ophtalmol.* **22**:201–204 (2007). doi:10.1080/08820530701543024.
6. T. Ghafourian, M. Barzegar-Jalali, S. Dastmalchi, T. Khavari-Khorasani, N. Hakimiha, and A. Nokhodchi. QSPR models for the prediction of apparent volume of distribution. *Int. J. Pharm.* **319**:82–97 (2006). doi:10.1016/j.ijpharm.2006.03.043.
7. T. Wajima, K. Fukumura, Y. Yano, and T. Oguma. Prediction of human clearance from animal data and molecular structural parameters using multivariate regression analysis. *J. Pharm. Sci.* **91**:2489–2499 (2002). doi:10.1002/jps.10242.
8. A. Cheng, and K. M. Merz Jr. Prediction of aqueous solubility of a diverse set of compounds using quantitative structure–property relationships. *J. Med. Chem.* **46**:3572–3580 (2003). doi:10.1021/jm020266b.
9. M. P. Gleeson. Plasma protein binding affinity and its relationship to molecular structure: an in-silico analysis. *J. Med. Chem.* **50**:101–112 (2007). doi:10.1021/jm060981b.
10. R. D. Schoenwald, and H. S. Huang. Corneal penetration behavior of beta-blocking agents I: physiochemical factors. *J. Pharm. Sci.* **72**:1266–1272 (1983). doi:10.1002/jps.2600721108.
11. F. Yoshida, and J. G. Topliss. Unified model for the corneal permeability of related and diverse compounds with respect to their physicochemical properties. *J. Pharm. Sci.* **85**:819–823 (1996). doi:10.1021/js960076m.
12. M. R. Prausnitz, and J. S. Noonan. Permeability of cornea, sclera, and conjunctiva: a literature analysis for drug delivery to the eye. *J. Pharm. Sci.* **87**:1479–188 (1998). doi:10.1021/js9802594.
13. Y. Li, J. Liu, D. Pan, and A. J. Hopfinger. A study of the relationship between cornea permeability and eye irritation using membrane-interaction QSAR analysis. *Toxicol. Sci.* **88**:434–446 (2005). doi:10.1093/toxsci/kfi319.
14. C. Chen, and J. Yang. MI-QSAR models for prediction of corneal permeability of organic compounds. *Acta Pharmacol. Sin.* **27**:193–204 (2006). doi:10.1111/j.1745-7254.2006.00241.x.
15. P. Saha, T. Uchiyama, K. J. Kim, and V. H. Lee. Permeability characteristics of primary cultured rabbit conjunctival epithelial cells to low molecular weight drugs. *Curr. Eye Res.* **15**:1170–1174 (1996). doi:10.3109/02713689608995152.
16. Y. Horibe, K. Hosoya, K. J. Kim, T. Ogiso, and V. H. Lee. Polar solute transport across the pigmented rabbit conjunctiva: size dependence and the influence of 8-bromo cyclic adenosine monophosphate. *Pharm. Res.* **14**:1246–1251 (1997). doi:10.1023/A:1012123411343.
17. L. Pitkanen, V. P. Ranta, H. Moilanen, and A. Urtti. Permeability of retinal pigment epithelium: effects of permeant molecular weight and lipophilicity. *Invest. Ophthalmol. Vis. Sci.* **46**:641–646 (2005). doi:10.1167/iovs.04-1051.
18. D. Maurice. Injection of Drugs into the vitreous body. In I. H. Leopold, and R. P. Burns (eds.), Symposium on Ocular Therapy, John Wiley, New York, 1976, pp. 59–72.
19. S. Mishima, and D. M. Maurice. Ocular pharmacokinetics. In M. L. Saers (ed.), *Handbook of Experimental Pharmacology, Vol. 59*, Springer, Berlin, 1984, pp. 16–119.
20. A. Ohtori, and K. Tojo. *In vivo*/*in vitro* correlation of intravitreal delivery of drugs with the help of computer simulation. *Biol. Pharm. Bull.* **17**:283–290 (1994).
21. S. Friedrich, Y. L. Cheng, and B. Saville. Finite element modeling of drug distribution in the vitreous humor of the rabbit eye. *Ann. Biomed. Eng.* **25**:303–14 (1997). doi:10.1007/BF02648045.
22. P. J. Missel. Hydraulic flow and vascular clearance influences on intravitreal drug delivery. *Pharm. Res.* **19**:1636–1647 (2002). doi:10.1023/A:1020940927675.
23. P. J. Missel. Finite and infinitesimal representations of the vasculature: ocular drug clearance by vascular and hydraulic effects. *Ann. Biomed. Eng.* **30**:1128–1139 (2002). doi:10.1114/1.1521417.
24. J. Xu, J. J. Heys, V. H. Barocas, and T. W. Randolph. Permeability and diffusion in vitreous humor: implications for drug delivery. *Pharm. Res.* **17**:664–669 (2000). doi:10.1023/A:1007517912927.
25. M. S. Stay, J. Xu, T. W. Randolph, and V. H. Barocas. Computer simulation of convective and diffusive transport of controlled-release drugs in the vitreous humor. *Pharm. Res.* **20**:96–102 (2003). doi:10.1023/A:1022207026982.
26. W. Liu, Q. F. Liu, R. Perkins, G. Drusano, A. Louie, A. Madu, U. Mian, M. Mayers, and M. H. Miller. Pharmacokinetics of sparfloxacin in the serum and vitreous humor of rabbits: physicochemical properties that regulate penetration of quinolone antimicrobials. *Antimicrob. Agents Chemother.* **42**:1417–1423 (1998).
27. C. S. Dias, and A. K. Mitra. Vitreal elimination kinetics of large molecular weight FITC-labeled dextrans in albino rabbits using a novel microsampling technique. *J. Pharm. Sci.* **89**:572–578 (2000). doi:10.1002/(SICI)1520-6017(200005)89:5<572::AID-JPS2>3.0.CO;2-P.
28. D. Maurice. Review: practical issues in intravitreal drug delivery. *J. Ocular Pharmacol. Ther.* **17**:393–401 (2001). doi:10.1089/108076801753162807.
29. B. H. Doft, J. Weiskopf, I. Nilsson-Ehle, and L. B. Wingard Jr. Amphotericin clearance in vitrectomized *versus* nonvitrectomized eyes. *Ophthalmology.* **92**:1601–1605 (1985).
30. L. B. Wingard Jr., J. J. Zuravleff, B. H. Doft, L. Berk, and J. Rinkoff. Intraocular distribution of intravitreally administered amphotericin B in normal and vitrectomized eyes. *Invest. Ophthalmol. Vis. Sci.* **30**:2184–2189 (1989).
31. H. S. Chin, T. S. Park, Y. S. Moon, and J. H. Oh. Difference in clearance of intravitreal triamcinolone acetonide between vitrectomized and nonvitrectomized eyes. *Retina*. **25**:556–560 (2005). doi:10.1097/00006982-200507000-00002.
32. G. N. Scholes, W. J. O'Brien, G. W. Abrams, and M. F. Kubicek. Clearance of triamcinolone from vitreous. *Arch. Ophthalmol.* **103**:1567–1569 (1985).
33. J. Ambati, C. S. Canakis, J. W. Miller, E. S. Gragoudas, A. Edwards, D. J. Weissgold, I. Kim, F. C. Delori, and A. P. Adamis. Diffusion of high molecular weight compounds through sclera. *Invest. Ophthalmol. Vis. Sci.* **41**:1181–1185 (2000).
34. A. C. Amrite, H. F. Edelhauser, and U. B. Kompella. Modeling of corneal and retinal pharmacokinetics after periocular drug administration. *Invest. Ophthalmol. Vis. Sci.* **49**:320–332 (2008). doi:10.1167/iovs.07-0593.
35. H. Atluri, and A. K. Mitra. Disposition of short-chain aliphatic alcohols in rabbit vitreous by ocular microdialysis. *Exp. Eye Res.* **76**:315–320 (2003). doi:10.1016/S0014-4835(02)00311-1.
36. P. M. Hughes, R. Krishnamoorthy, and A. K. Mitra. Vitreous disposition of two acycloguanosine antivirals in the albino and pigmented rabbit models: a novel ocular microdialysis technique. *J. Ocular Pharmacol. Ther.* **12**:209–224 (1996).
37. G. Peyman, D. Sanders, and M. Goldberg. *Advances in uveal surgery, vitreous surgery, and the treatment of edophthalmitis*. Appleton-Century-Crofts, New York, 1975.
38. H. J. Koh, L. Cheng, K. Bessho, T. R. Jones, M. C. Davidson, and W. R. Freeman. Intraocular properties of urokinase-derived antiangiogenic A6 peptide in rabbits. *J. Ocular Pharmacol. Ther.* **20**:439–449 (2004).
39. A. G. Schenk, G. A. Peyman, and J. T. Paque. The intravitreal use of carbenicillin (Geopen) for treatment od pseudomonas endophthalmitis. *Acta Ophthalmol. (Copenh)*. **52**:707–717 (1974).
40. S. Macha, and A. K. Mitra. Ocular pharmacokinetics of cephalosporins using microdialysis. *J. Ocular Pharmacol. Ther.* **17**:485–498 (2001). doi:10.1089/108076801753266866.
41. W. M. Jay, P. Fishman, M. Aziz, and R. K. Shockley. Intravitreal ceftazidime in a rabbit model: dose- and time-dependent toxicity and pharmacokinetic analysis. *J. Ocul. Pharmacol.* **3**:257–262 (1987).
42. R. K. Shockley, W. M. Jay, T. R. Friberg, A. M. Aziz, J. P. Rissing, and M. Z. Aziz. Intravitreal ceftriaxone in a rabbit model. Dose- and time-dependent toxic effects and pharmacokinetic analysis. *Arch Ophthalmol.* **102**:1236–1238 (1984).
43. K. C. Cundy, G. Lynch, J. P. Shaw, M. J. Hitchcock, and W. A. Lee. Distribution and metabolism of intravitreal cidofovir and cyclic HPMPC in rabbits. *Curr. Eye Res.* **15**:569–576 (1996). doi:10.3109/02713689609000768.
44. M. Unal, G. A. Peyman, C. Liang, H. Hegazy, L. C. Molinari, J. Chen, S. Brun, and P. J. Tarcha. Ocular toxicity of intravitreal clarithromycin. *Retina*. **19**:442–446 (1999). doi:10.1097/00006982-199909000-00013.

45. R. Fiscella, G. A. Peyman, and P. H. Fishman. Duration of therapeutic levels of intravitreally injected liposome-encapsulated clindamycin in the rabbit. *Can. J. Ophthalmol.* **22**:307–309 (1987).
46. P. A. Pearson, G. J. Jaffe, D. F. Martin, G. J. Cordahi, H. Grossniklaus, E. T. Schmeisser, and P. Ashton. Evaluation of a delivery system providing long-term release of cyclosporine. *Arch. Ophthalmol.* **114**:311–317 (1996).
47. H. I. Meisels, and G. A. Peyman. Intravitreal erythromycin in the treatment of induced staphylococcal endophthalmitis. *Ann. Ophthalmol.* **8**:939–943 (1976).
48. S. K. Gupta, T. Velpandian, N. Dhingra, and J. Jaiswal. Intravitreal pharmacokinetics of plain and liposome-entrapped fluconazole in rabbit eyes. *J. Ocular Pharmacol. Ther.* **16**:511–518 (2000).
49. B. S. Anand, H. Atluri, and A. K. Mitra. Validation of an ocular microdialysis technique in rabbits with permanently implanted vitreous probes: systemic and intravitreal pharmacokinetics of fluorescein. *Int. J. Pharm.* **281**:79–88 (2004). doi:10.1016/j.ijpharm.2004.05.028.
50. P. Berthe, C. Baudouin, R. Garraffo, P. Hofmann, A. M. Taburet, and P. Lapalus. Toxicologic and pharmacokinetic analysis of intravitreal injections of foscarnet, either alone or in combination with ganciclovir. *Invest. Ophthalmol. Vis. Sci.* **35**:1038–1045 (1994).
51. S. Macha, and A. K. Mitra. Ocular disposition of ganciclovir and its monoester prodrugs following intravitreal administration using microdialysis. *Drug Metab. Dispos.* **30**:670–675 (2002). doi:10.1124/dmd.30.6.670.
52. G. A. Peyman, D. R. May, E. S. Ericson, and D. Apple. Intraocular injection of gentamicin. Toxic effects of clearance. *Arch. Ophthalmol.* **92**:42–47 (1974).
53. C. Solans, M. A. Bregante, M. A. Garcia, and S. Perez. Ocular penetration of grepafloxacin after intravitreal administration in albino and pigmented rabbits. *Chemotherapy.* **50**:133–137 (2004). doi:10.1159/000077887.
54. J. M. Leeds, S. P. Henry, L. Truong, A. Zutshi, A. A. Levin, and D. Kornbrust. Pharmacokinetics of a potential human cytomegalovirus therapeutic, a phosphorothioate oligonucleotide, after intravitreal injection in the rabbit. *Drug Metab. Dispos.* **25**:921–926 (1997).
55. A. G. Schenk, and G. A. Peyman. Lincomycin by direct intravitreal injection in the treatment of experimental bacterial endophthalmitis. *Albrecht Von Graefes Arch. Klin. Exp. Ophthalmol.* **190**:281–291 (1974). doi:10.1007/BF00407889.
56. G. Velez, P. Yuan, C. Sung, G. Tansey, G. F. Reed, C. C. Chan, R. B. Nussenblatt, and M. R. Robinson. Pharmacokinetics and toxicity of intravitreal chemotherapy for primary intraocular lymphoma. *Arch. Ophthalmol.* **119**:1518–1524 (2001).
57. N. H. Leeds, G. A. Peyman, and B. House. Moxalactam (Moxam) in the treatment of experimental staphylococcal endophthalmitis. *Ophthalmic. Surg.* **13**:653–656 (1982).
58. S. Duvvuri, M. D. Gandhi, and A. K. Mitra. Effect of P-glycoprotein on the ocular disposition of a model substrate, quinidine. *Curr. Eye Res.* **27**:345–353 (2003). doi:10.1076/ceyr.27.6.345.18187.
59. H. Kim, K. G. Csaky, C. C. Chan, P. M. Bungay, R. J. Lutz, R. L. Dedrick, P. Yuan, J. Rosenberg, A. J. Grillo-Lopez, W. H. Wilson, and M. R. Robinson. The pharmacokinetics of rituximab following an intravitreal injection. *Exp. Eye Res.* **82**:760–766 (2006). doi:10.1016/j.exer.2005.09.018.
60. E. K. Kim, and H. B. Kim. Pharmacokinetics of intravitreally injected liposome-encapsulated tobramycin in normal rabbits. *Yonsei Med. J.* **31**:308–314 (1990).
61. H. Kim, K. G. Csaky, L. Gravlin, P. Yuan, R. J. Lutz, P. M. Bungay, G. Tansey, D. E. F. Monasterio, G. K. Potti, G. Grimes, and M. R. Robinson. Safety and pharmacokinetics of a preservative-free triamcinolone acetonide formulation for intravitreal administration. *Retina.* **26**:523–530 (2006). doi:10.1097/00006982-200605000-00005.
62. M. P. Pang, R. V. Branchflower, A. T. Chang, G. A. Peyman, H. Blatt, and H. K. Minatoya. Half-life and vitreous clearance of trifluorothymidine after intravitreal injection in the rabbit eye. *Can. J. Ophthalmol.* **27**:6–9 (1992).
63. M. A. Smith, J. A. Sorenson, C. Smith, M. Miller, and M. Borenstein. Effects of intravitreal dexamethasone on concentration of intravitreal vancomycin in experimental methicillin-resistant Staphylococcus epidermidis endophthalmitis. *Antimicrob. Agents Chemother.* **35**:1298–1302 (1991).
64. Y. C. Shen, M. Y. Wang, C. Y. Wang, T. C. Tsai, H. Y. Tsai, Y. F. Lee, and L. C. Wei. Clearance of intravitreal voriconazole. *Invest. Ophthalmol. Vis. Sci.* **48**:2238–2241 (2007). doi:10.1167/iovs.06-1362.
65. D. S. Wishart, C. Knox, A. C. Guo, S. Shrivastava, M. Hassanali, P. Stothard, Z. Chang, and J. Woolsey. DrugBank: a comprehensive resource for in silico drug discovery and exploration. *Nucleic Acids Res.* **34**:D668–D672 (2006). doi:10.1093/nar/gkj067.
66. M. Barza, and M. McCue. Pharmacokinetics of aztreonam in rabbit eyes. *Antimicrob. Agents Chemother.* **24**:468–473 (1983).
67. S. J. Bakri, M. R. Snyder, J. M. Reid, J. S. Pulido, and R. J. Singh. Pharmacokinetics of intravitreal bevacizumab (Avastin). *Ophthalmology.* **114**:855–859 (2007). doi:10.1016/j.ophtha.2007.01.017.
68. M. Barza, A. Kane, and J. Baum. The effects of infection and probenecid on the transport of carbenicillin from the rabbit vitreous humor. *Invest. Ophthalmol. Vis. Sci.* **22**:720–726 (1982).
69. J. P. Fisher, S. E. Civiletto, and R. K. Forster. Toxicity, efficacy, and clearance of intravitreally injected of cefazolin. *Arch. Ophthalmol.* **100**:650–652 (1982).
70. W. M. Jay, and R. K. Shockley. Toxicity and pharmacokinetics of cefepime (BMY-28142) following intravitreal injection in pigmented rabbit eyes. *J. Ocul. Pharmacol.* **4**:345–349 (1988).
71. M. Barza, E. Lynch, and J. L. Baum. Pharmacokinetics of newer cephalosporins after subconjunctival and intravitreal injection in rabbits. *Arch. Ophthalmol.* **111**:121–125 (1993).
72. H. W. Kwak, and D. J. D'Amico. Evaluation of the retinal toxicity and pharmacokinetics of dexamethasone after intravitreal injection. *Arch. Ophthalmol.* **110**:259–266 (1992).
73. S. Fauser, H. Kalbacher, N. Alteheld, K. Koizumi, T. U. Krohne, and A. M. Joussen. Pharmacokinetics and safety of intravitreally delivered etanercept. *Graefes Arch. Clin. Exp. Ophthalmol.* **242**:582–586 (2004). doi:10.1007/s00417-004-0895-x.
74. L. F. Lopez-Cortes, M. T. Pastor-Ramos, R. Ruiz-Valderas, E. Cordero, A. Uceda-Montanes, C. M. Claro-Cala, and M. J. Lucero-Munoz. Intravitreal pharmacokinetics and retinal concentrations of ganciclovir and foscarnet after intravitreal administration in rabbits. *Invest. Ophthalmol. Vis. Sci.* **42**:1024–1028 (2001).
75. A. Kane, M. Barza, and J. Baum. Intravitreal injection of gentamicin in rabbits. Effect of inflammation and pigmentation on half-life and ocular distribution. *Invest. Ophthalmol. Vis. Sci.* **20**:593–597 (1981).
76. S. Perez, C. Solans, M. A. Bregante, I. Pinilla, M. A. Garcia, and F. Honrubia. Pharmacokinetics and ocular penetration of grepafloxacin in albino and pigmented rabbits. *J. Antimicrob. Chemother.* **50**:541–545 (2002). doi:10.1093/jac/dkf178.
77. J. C. Veltman, J. Podval, J. Mattern, K. L. Hall, R. J. Lambert, and H. F. Edelhauser. The disposition and bioavailability of 35S-GSH from 35S-GSSG in BSS PLUS in rabbit ocular tissues. *J. Ocular Pharmacol. Ther.* **20**:256–268 (2004). doi:10.1089/1080768041223639.
78. M. N. Iyer, F. He, T. G. Wensel, W. F. Mieler, M. S. Benz, and E. R. Holz. Clearance of intravitreal moxifloxacin. *Invest. Ophthalmol. Vis. Sci.* **47**:317–319 (2006). doi:10.1167/iovs.05-1124.
79. R. M. Coco, M. I. Lopez, J. C. Pastor, and M. J. Nozal. Pharmacokinetics of intravitreal vancomycin in normal and infected rabbit eyes. *J. Ocular Pharmacol. Ther.* **14**:555–563 (1998).